Journal Pre-proof

Thermochronology of the Ventana Ranges and Claromecó Basin, Argentina: Record of Gondwana breakup and South Atlantic passive margin dynamics

Arzadún Guadalupe, Lovecchio Juan Pablo, Becchio Raúl, Uriz Norberto Javier, Cingolani Carlos, Febbo María Belén, Hernandez Roberto, Bolatti Nestor, Kress Pedro

PII: S0895-9811(20)30508-3

DOI: https://doi.org/10.1016/j.jsames.2020.102965

Reference: SAMES 102965

To appear in: *Journal of South American Earth Sciences*

Received Date: 17 June 2020

Revised Date: 5 October 2020

Accepted Date: 14 October 2020

Please cite this article as: Guadalupe, Arzadú., Pablo, L.J., Raúl, B., Javier, U.N., Carlos, C., Belén, Febbo.Marí., Roberto, H., Nestor, B., Pedro, K., Thermochronology of the Ventana Ranges and Claromecó Basin, Argentina: Record of Gondwana breakup and South Atlantic passive margin dynamics, *Journal of South American Earth Sciences* (2020), doi: https://doi.org/10.1016/j.jsames.2020.102965.

Thermochronology of the Ventana Ranges and Claromecó Basin, Argentina: Record of Gondwana breakup and South Atlantic passive margin dynamics

Arzadún Guadalupe[1,2], Lovecchio Juan Pablo[3], Becchio Raúl[1,4], Uriz Norberto Javier[5], Cingolani Carlos[1,5], Febbo María Belén[6,7], Hernandez Roberto[2], Bolatti Nestor[3], Kress Pedro[3]

[1]Consejo Nacional de Investigaciones Científicas y Técnicas (CONICET), Argentina
[2]Laboratorio de Termocronología (LaTe Andes). Las Moreras 510, Vaqueros, Salta, Argentina
[3]YPF S.A. Exploration. Macacha Güemes 515, 1106, Buenos Aires, Argentina
[4]Universidad Nacional de Salta, Argentina
[5]Universidad Nacional de La Plata, Argentina
[6]Comisión de Investigaciones Científicas de la Provincia de Buenos Aires (CIC), Argentina
[7]Departamento de Geología, Universidad Nacional del Sur, Bahía Blanca, Argentina

Abstract

The Ventana Ranges and the neighboring Claromecó basin display multiple extensional and compressional tectonic events throughout their Phanerozoic evolution. A passive continental margin setting during the early Paleozoic changed to a compressional system in the late Paleozoic, for which the Ventana Ranges are its fossilized fold and thrust belt and the Claromecó Basin, to the north-northeast, its associated foreland basin. The thermochronology study presented here and the cooling ages obtained for the Ventana Ranges are interpreted as a long-lived, probably multi-stage, exhumation event that occurred throughout the Mesozoic. The ZFT and AFT ages indicate that the Silurian, Devonian, Carboniferous and Permian units cooled during the Late Triassic to Early Jurassic (from 204.4 ± 18.8 to 146.5 ± 11.6 Ma). These ages, consistent with rifting events described for the neighboring Colorado basin (to the south-southeast), are interpreted as exhumation in the rift's northern flank. In the Claromecó Basin, a cooling event is indicated from the AFT PAZ data for the late Early Cretaceous (Barremian-Aptian, 125.8 ± 10.6 Ma), interpreted as a part of passive margin exhumation during the drift stage after the South Atlantic opening in the Valanginian-Hauterivian. The obtained ages indicate exhumation in the basin flank and are consistent with the different rifting events previously interpreted for Colorado basin.

Keywords: Ventana Ranges, Claromecó basin, thermochronology, Colorado basin, Gondwana breakup

1. Introduction

The exhumation and subsidence processes that characterize the evolution of passive margins are also recorded onshore and can be deduced from the dynamics of coastal rock massifs (e.g. Japsen *et al*., 2012; Hueck *et al*., 2017; Krob *et al.*, 2020). Low-temperature thermochronology provides cooling ages that allow an assessment of the thermal history of the sedimentary basins (Malusà and Fitzgerald, 2019). In this paper, cooling ages are obtained from apatite and zircon fission tracks for different stratigraphic units in the Ventana Ranges and Claromecó Basin (onshore Argentina). These data are integrated with previous thermal data obtained from fluid inclusion and vitrinite reflectance and correlated with existing paleomagnetic and geochronological data, with reassessing the Argentinean passive margin evolution during the South Atlantic rifting and breakup.

The Ventana Ranges (Sierras Australes of Buenos Aires, 37º-39º S and 61º-63º W, Fig. 1), expose an Early-to-Late Paleozoic succession that records multiple compressional and extensional tectonic events throughout its Phanerozoic evolution. In the early Paleozoic, this region was part of a passive margin along the southwestern margin of the Gondwana supercontinent (Keidel, 1916; Harrington, 1947; Suero, 1972; Kilmurray, 1975; Von Gosen *et al*., 1990). In the late Paleozoic, this margin was part of a subducting plate that collided with the Patagonia terrain during the Permian as part of the Gondwanide orogeny (Ramos, 1984), in a model that is still under debate (see Tomezzoli, 2012). Therefore, a fold-and-thrust belt and an associated foreland basin developed to the north of the suture with Patagonia, both on the South American and African plates. The fold-and-thrust belt is represented by the Ventana Ranges in South America and by the Cape system (du Toit, 1921; Hälbich, 1981) in South Africa. The associated foreland basins are the Claromecó basin (Kostadinoff and Prozzi, 1998; Lesta and Sylwan, 2005; Pángaro and Ramos, 2012, Pángaro *et al.*, 2015) and the Karoo Basin, respectively (du Toit, 1927; Catuneanu *et al*., 2005). This system has been reassessed by Pángaro *et al.* (2016) and unified in the Permo-Triassic Hesperides basin.

During the Mesozoic, several rifting events affected this area with the formation of the Colorado basin offshore Argentina (Fig. 1, Lovecchio *et al*., 2018; 2020). This extensional history ended the breakup along the South Atlantic margin in the Early Cretaceous. The Late Cretaceous and Cenozoic evolution is marked by drifting of the South American plate and the South Atlantic passive margin evolution.

The interpretation of exhumation data, particularly in the Ventana Ranges, is challenging because the morphology and processes are strongly affected by the Paleozoic structure. Burmistrov (1971) and Selles Martinez (2001) propose an exhumation event during the Jurassic-Cretaceous, where the Ranges would act as a horst limited by normal faults. However, with limited outcrop and subsurface data, these interpretations remain under discussion.

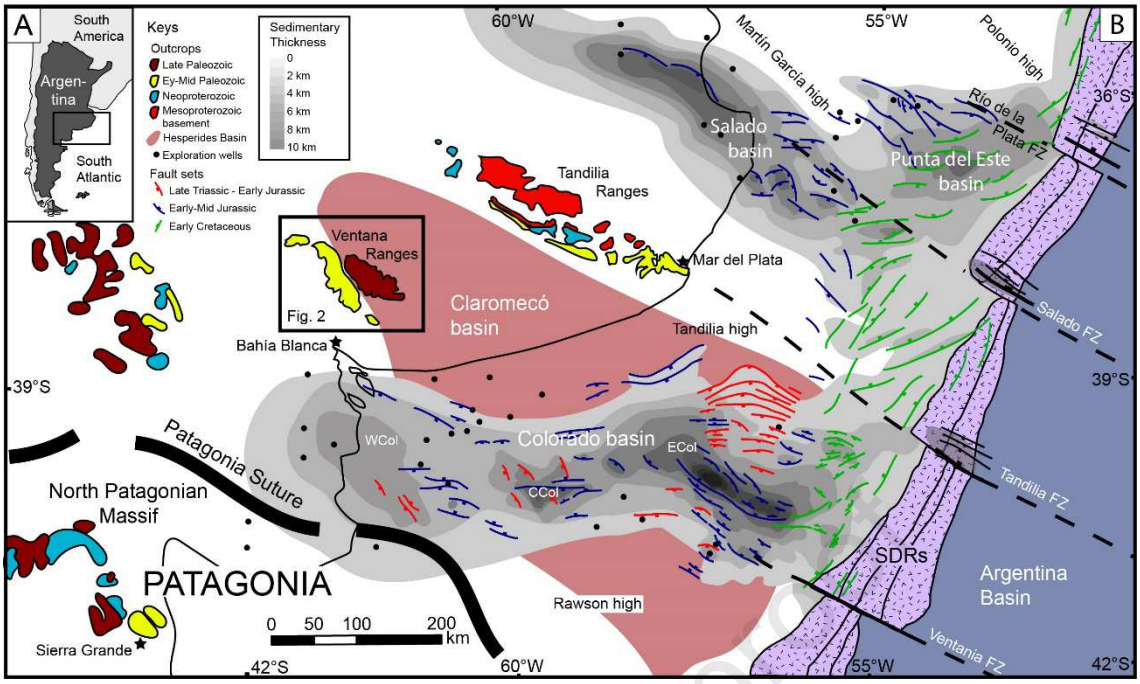

Figure 1. Location map of the study area in central-eastern Argentina. The map shows the superposition of the Claromecó Basin developed onshore and extending to the SE, and the E-W oriented Colorado basin offshore Argentina. Modified from Lovecchio et al. (2018) after Pángaro and Ramos (2012).

2. Geological Framework

a. Paleozoic Evolution

The Ventana Ranges represent a fossilized fold and thrust belt with northeast vergence, involving Lower and Upper Paleozoic series (Harrington, 1980; Von Gosen *et al.*, 1991; Tomezzoli and Cristallini, 1998, 2004) (Figs. 1 and 2). The entire sedimentary succession involved in the deformation reaches around 4,500 m in thickness (Ramos et al., 2014). The oldest units crop out on its western flank, with the presence of younger units to the east. The succession has been divided in three groups, from west to east: Curamalal, Ventana and Pillahuincó (Fig. 2) that display an important variation in the degree of metamorphism and style of deformation (Harrington, 1947). The early Paleozoic Curamalal and Ventana Groups, to the west, display a lower greenschist metamorphism (Cobbold *et al.*, 1986; Buggisch, 1987), while in the late Paleozoic Pillahuincó Group, to the east, the sedimentary successions are still in the diagenesis range (Iñiguez Rodriguez and Andreis, 1971; Buggish, 1987; Von Gosen *et al.*, 1989). The deformation is also more intense in the western sector, in the Curamalal, Bravard and Ventana Ranges, while the eastern sector (Las Tunas and Pillahuincó Ranges) is characterized by a more open folding (Fig. 2C).

The Claromecó Basin is a late Paleozoic foreland developed in the southwestern margin of Gondwana, between the Río de la Plata craton (exposed in the Tandilia Ranges) and the Ventana fold and thrust belt (Fig. 1). The structural evolution of the basin was associated to the collision of the Patagonia terrane with the southwestern

Gondwana margin (Ramos, 1984; Kostadinoff and Prozzi, 1998; Ramos, 1999; Lesta and Sylwan, 2005; Pángaro and Ramos, 2012). The late Paleozoic series deposited in the Claromecó Basin, crop out in the Pillahuincó ranges (Ramos and Kostadinoff 2005, Zorzano *et al.* 2011; Fig. 2A) and are also present offshore in the prerift of the Colorado Basin (Lesta *et al.*, 1978) in what has recently been described by Pángaro *et al*. (2016) as the Hesperides basin (Fig. 1).

The succession starts with the Cambrian-Ordovician Curamalal Group, which represents a siliciclastic passive margin dominated by the deposition of fine-grained sandstones (Harrington, 1947) (Fig. 1). The Curamalal Group is unconformably overlaid by the Ventana Group, which starts with the Bravard Formation coarse-to-conglomeratic sandstones, followed by the deposition of the Napostá, Formation, which displays thicknesses ranging from 420 to 600 m (Harrington, 1947; Andreis, 1965) and is composed of fine-grained quartz-rich sandstones (Harrington, 1947). An Ordovician to Silurian age is suggested for the Napostá Fm from its ichnofossil content (Dimieri and Japas, 1986; Buggisch, 1986, 1987; Rodríguez 1988; Seilacher *et al.* 2002). Quartz-rich sandstones of the Providencia Formation conformably overlay the Napostá Formation, with a thickness of 200 to 300 m (Harrington, 1947). Follows the Lolén Formation with a thickness of 600 m and composed of sandstones and siltstones interbedded with lenticular fine-grained conglomerates (Harrington, 1972). Paleontological content indicates a Middle Devonian age (Keidel, 1916; Harrington, 1947; Andreis *et al.,* 1989; Cingolani *et al.,* 2002) (Fig. 3).

The nature of the contact between the Ventana Group and the overlying Pillahuincó Group is controversial; nevertheless, the presence of a regional unconformity is generally accepted (Harrington, 1947; Japas, 1988; Massabie and Rossello, 1984; Tomezzoli, 1997; Tomezzoli and Cristallini, 1998).

The Pillahuincó Group is formed by the Sauce Grande, Piedra Azul, Bonete and Tunas formations, and is interpreted to record the formation and filling of a foreland basin (Harrington, 1947). The succession starts with the Sauce Grande Formation displaying a thickness of 1,100 m, composed of diamictites (Coates, 1969; Harrington, 1980; Andreis, 1984), sandstones and a minor proportion of mudstones (Andreis *et al.*, 1989), deposited in a glacial environment. Its palynological content indicates a Pennsylvanian-Cisuralian age (Di Pasquo *et al.*, 2008; Archangelsky *et al.,* 1987) (Fig. 3).

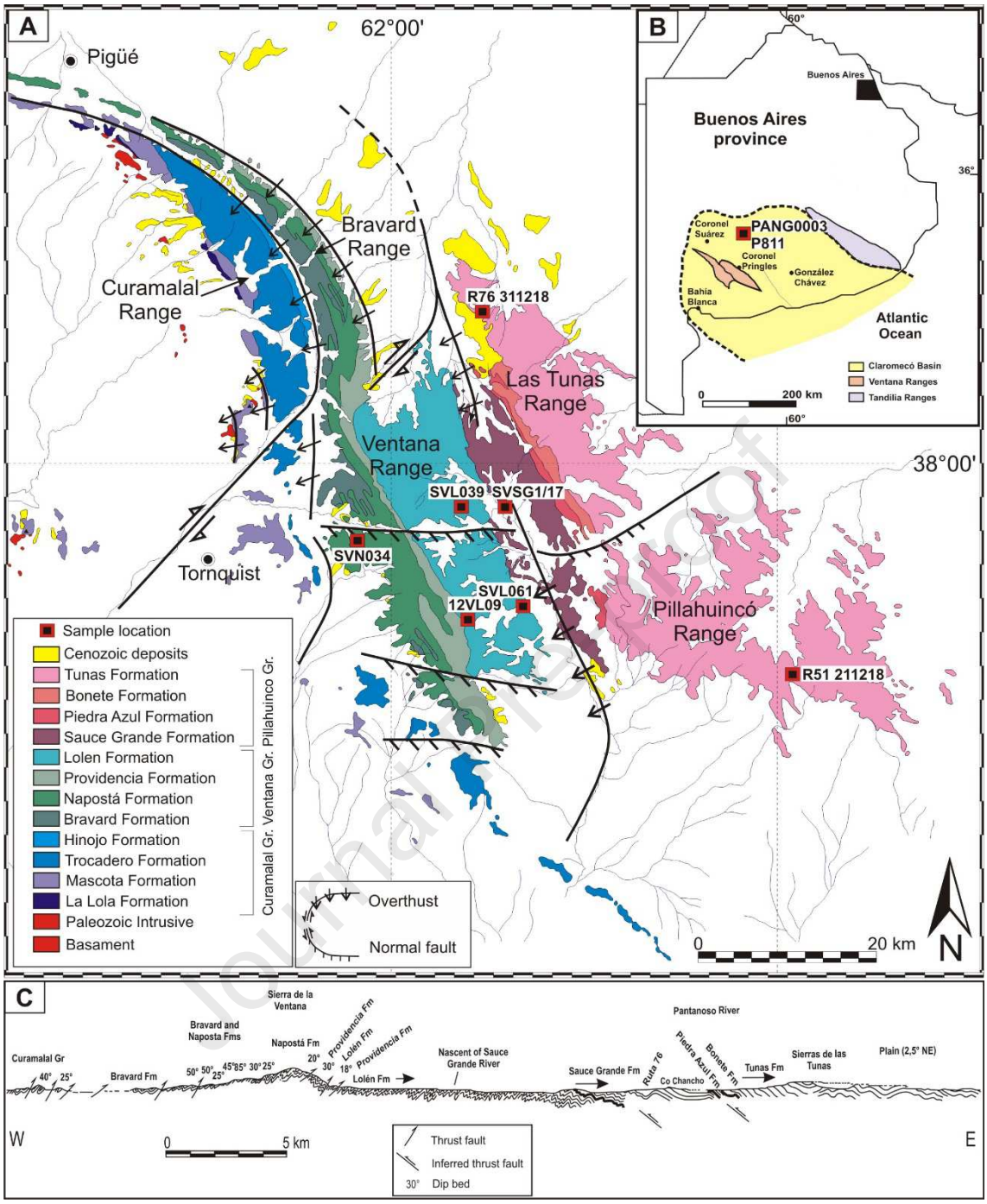

Figure 2. A: Geological map of the Ventana Ranges (see location in Fig. 1). Notice the location of the samples analyzed in this study; **B:** Location map highlighting the location of the PANG0003 well (sample P811) in the Claromecó Basin. Structure adapted from Cobbold *et al.* (1986). **C:** Structural section across the Ventana Ranges (modified from Tomezzoli and Cristallini, 2004).

The Sauce Grande Formation transitionally grades to the Piedra Azul Formation, composed of mudrocks and fine-grained sandstones deposited in a marine environment (López Gamundi, 1996; Andreis and Japas, 1996). The Bonete Formation (Harrington, 1947) conformably overlays the Piedra Azul Formation and is composed of a fine-

grained arkosic-sandstones and mudstones succession (Harrington, 1947), with paleofloral content suggesting an Early Permian age (Archangelsky and Cúneo, 1984). Conformably overlying, the Tunas Formation (Harrington, 1947) is composed of fine-to-medium-grained sandstones interbedded with siltstones (Andreis *et al.*, 1979; Andreis and Cladera, 1992; López Gamundi, 1996). An Early Permian age is suggested from its paleontological content: *Glossopteris Lycopsids*, and poorly preserved bivalves (Harrington, 1947; Furque, 1973; Ruiz and Bianco, 1985, Archangelsky and Cúneo, 1984). Evidence of coetaneous explosive volcanic activity and syn-sedimentary deformation is present in the Tunas Formation (Japas, 1986, 1988, Lopez Gamundi, 1995; Tomezzoli and Vilas, 1999; Tomezzoli, 2001; Ramos *et al*., 2014). Tuff levels intercalated in the Tunas Formation (Iñiguez *et al*., 1988) yielded U/Pb ages of 291 and 281 Ma (López Gamundi *et al.,* 2013; Alessandretti *et al.,* 2013; Ramos *et al.*, 2013; Arzadún *et al.*, 2018; Ballivián Justiniano *et al*., 2020). There are several discrepancies regarding the thickness of the Tunas Formation. Different authors measured thicknesses between 710 and 2,400 m in outcrop (Andreis *et al.*, 1979; Suero, 1972; Japas, 1986; Zorzano *et al.*, 2011) and more than 1000 m in the sub-surface (Zorzano *et al.*, 2011; Lesta and Sylwan, 2005) (Fig. 3).

A major unconformity is observed in the Claromecó basin at the top of the Tunas Formation, separating this unit from the unconformably overlaying Cenozoic deposits (Fig. 3).

Regarding the structure, thrust faulting commonly affects the Ventana and Pillahuincó Groups (Dimieri and Di Nardo, 1992; Tomezzoli and Cristallini, 1998) (Fig. 2c). Also, tear faults were described affecting the Ventana Group (Amos and Urien, 1968; Massabie and Rossello, 1984). Several authors consider that a single tectonic event affected the Paleozoic series of the Ventana Ranges and generated the folding and trusting (Harrington, 1947, 1972; Furque, 1973; Suero, 1972; Llambías and Prozzi, 1975; Ramos, 1984; Varela *et al.*, 1985; Sellés Martínez, 1986; Cobbold *et al*., 1987, 1991; von Gosen *et al*., 1989, 1990; Japas, 1995; López-Gamundí *et al.*, 1995; Rossello *et al*., 1997; Rapela *et al*., 2003; Tomezzoli and Cristallini, 2004). Rossello and Massabie (1981) consider that a later event, oriented in the NW-SE direction, was responsible for the curvature of the northwestern sector, while von Gosen *et al.* (1990) suggest, alternatively, that a transcurrent event produced the arcuate shape of the Ventana Ranges.

In the Curamalal and Ventana Ranges (placed to the west, Fig. 2A), the axial surface of the folds involving the Lolén and Sauce Grande formations and the axial plane foliations dip to the southwest. Toward the Pillahuincó Ranges (Fig. 2A), the folding is attenuated and the axial planes are vertical or dipping to the northeast, thus indicating a vergence change recorded in the syn-tectonic formations (Harrington, 1947, 1970; Furque, 1973; Japas, 1986; Tomezzoli and Cristallini, 1998, Arzadún *et al.*, 2017) (see Fig. 2C).

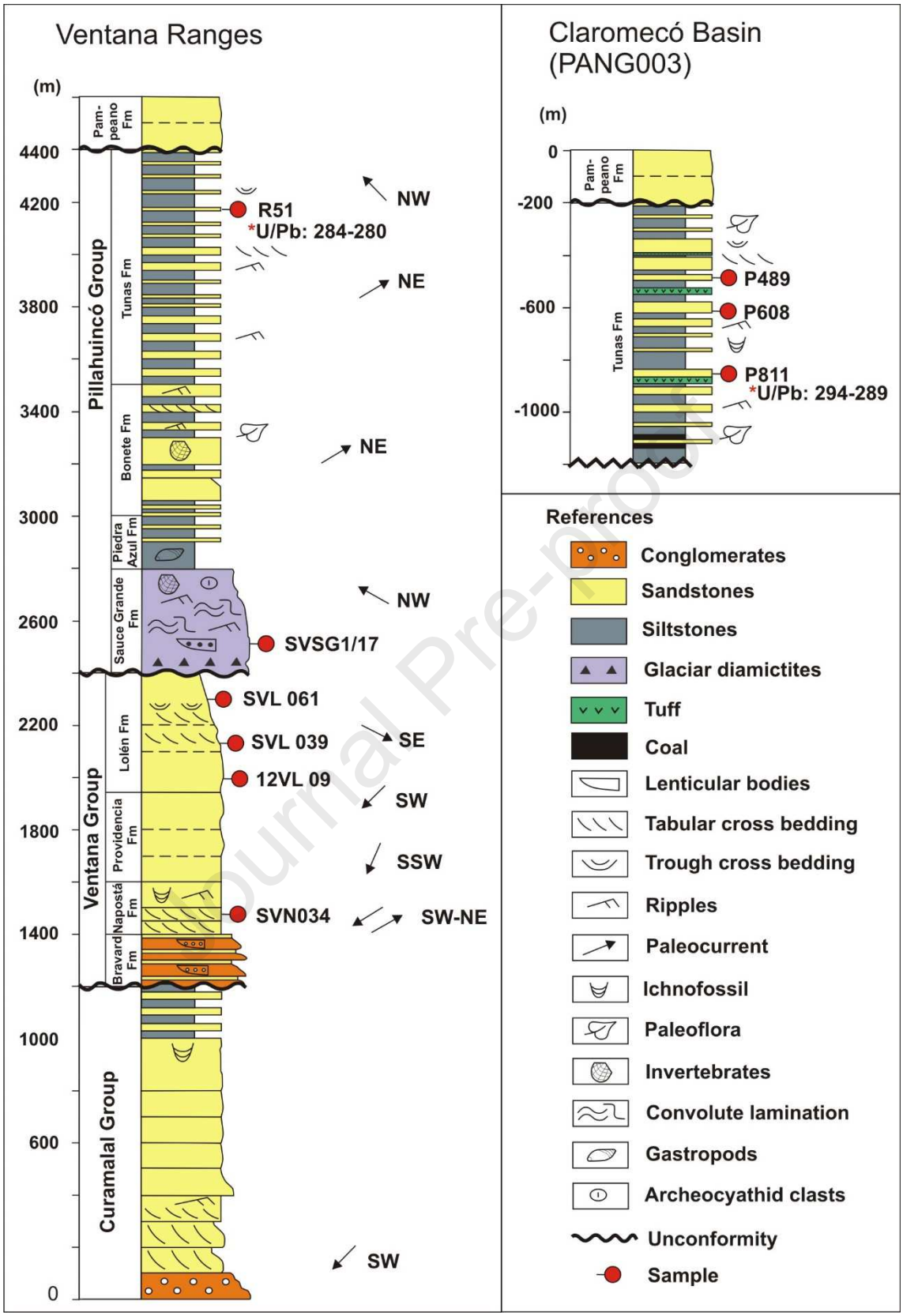

Figure 3. Stratigraphic column of the Paleozoic succession in the Ventana Ranges (modified from Ramos *et al.*, 2014) and of the Claromecó Basin in the PANG003 well. The location of the samples used in this study is depicted, together with available U/Pb ages (from Arzadún *et al.*, 2018).

Ramos (1984) and Ramos *et al.* (2013) interpreted that the Ventana Ranges are the product of the collision of the Patagonia terrane to the SW margin of Gondwana. Other authors explained the formation of the Ventana Ranges as a system of continental blocks affected by a tectonic event producing crustal fragmentation through strike-slip faults (Kostadinoff, 1993; Álvarez, 2004; Kostadinoff, 2007; Gregori *et al.*, 2003, 2008). Tomezzoli (2012) proposed that the deformation began in the Devonian-Carboniferous limit and continued throughout the Permian as the consequence of the combination of both processes.

b. Mesozoic Rifting History

The end of the Late Paleozoic Gondwanide orogeny (du Toit, 1927; Ramos, 2008), responsible for the formation of the Ventana and Cape fold belts, seems diachronous (Lopez Gamundi *et al.*, 1995; Tomezzoli, 2012). In South America, the last records of compression are the synorogenic Early to Middle Permian deposits of the Tunas Formation (Tomezzoli, 2001, Arzadún *et al*., 2017). In Africa, compression lasted until the Early Triassic (Hälbich, 1983; Hansma *et al*., 2016). After the end of the orogeny, generalized extension is interpreted in the area due to an absolute displacement of Pangea to the northeast, associated with counter-clockwise rotation of the supercontinent (Tomezzoli, 2001; Riel *et al*., 2018). A succession of rifting events throughout the Mesozoic was responsible for dismembering the ancient supercontinent of Gondwana (Uliana *et al.*, 1989; Frizon De Lamotte *et al*., 2015; Lovecchio *et al*., 2020).

South of the Ventana Ranges, the Colorado basin is an E-W extensional trough covering an area of more than 150,000 km^2 on the Argentinean shelf. It is limited by the Ventana and Tandilia Ranges to the north and by the Rawson High to the south (Gerster *et al*., 2011; Fig. 1). The evolution of the Colorado basin has been studied from seismic and hydrocarbon exploration well data (Kaasschieter, 1963; Lesta *et al.*, 1978; Fryklund *et al*., 1996; Juan *et al.*, 1996; Gerster *et al*., 2011; Autin *et al*., 2013; Loegering *et al*., 2013).

The Mesozoic rifting evolution of the Colorado basin has recently been reviewed by Lovecchio *et al.* (2018, 2020), who identified at least three Mesozoic extensional events, associated with different generations of faults and depocenter formation (Fig. 1). Assigning ages to the synrift infill of the different Colorado basin depocenters is challenging because they are poorly explored. Ages of rifting events are then interpreted from the geological framework and the evolution of neighboring basins (Lovecchio *et al.*, 2020). A first rifting event is interpreted to have occurred after the end of the Gondwanides orogeny, in the Late Triassic-Early Jurassic (red colored faults in Fig. 1). This event is correlated to the Precuyano cycle of the Neuquén basin (D'Elia *et al*., 2005; Mosquera *et al*., 2011). In the African counterpart, Muir *et al*. (2020) have recently published Early Jurassic U/Pb detrital zircon data from synrift deposits associated with extension in the Cape fold belt.

Following a first rifting stage in the Late Triassic-Early Jurassic, the Colorado basin area would have been affected by a second rifting event in the Early-to-Mid

Jurassic, with the formation of the main Colorado basin depocenters, especially the Central (CCol) and Eastern (ECol) depocenters (Fig. 1). This rifting event was correlated to the Early-Middle Jurassic Karoo rifting (Lovecchio *et al*., 2020). In the Early Cretaceous, a final rifting event, E-W oriented, produced breakup and the opening of the South Atlantic Ocean. A third generation of faults identified in the Colorado basin area, particularly developed to the east of the basin and was correlated with the Early Cretaceous South Atlantic rifting event (green colored faults in Fig. 1).

The understanding of the Mesozoic rifting events is important for the correct interpretation of the thermochronological evolution of the Ventana Ranges in particular and the SW Gondwana margin in general, as this area acted as a northern flank of the Colorado basin and would have experienced exhumation during the different rifting events. A first attempt in the understanding of the exhumation history of the study area was performed by Kollenz *et al.* (2016), who carried out AFT, and (U-Th-Sm)/He in zircon and apatite, and obtained Late Triassic to Late Cretaceous cooling ages for the Precambrian to Permian units in the Ventana Ranges.

3. Materials and Methods

The "fission track thermochronology" is based on the radioactive decay by natural spontaneous fission of uranium 238 (^{238}U), where each fission generates a track (Wagner, 1992). The fission tracks are generated with a constant velocity over geologic time, so the number of fission tracks in a mineral depends on the time lapsed and the uranium content of the grain. Fission track thermocronology can be carried out on apatite and zircon grains (AFT and ZFT respectively). The data obtained indicate the cooling ages of the apatite and zircons, at certain temperatures referred to as closing temperature (Tc) that is 100 ± 10°C in AFT (Green and Durrani, 1977), and 200-300° in ZFT (Zaun and Wagner, 1985; Tagami *et al.*, 1996, 1998; Yamada *et al*., 1993, 1995, 2007; Tagami and Shimada, 1996; Garver, 2002, 2003; Rahn *et al*., 2004; Reiners and Brandon, 2006). Each mineral is metastably related to time and temperature and has a "total annealing" temperature in which the tracks shorten to disappear in 10 My. The "partial annealing zone" (PAZ, Gleadow and Fitzgerald, 1987) corresponds to 60 to 110°C in apatites and 200 to 300° in zircons (Zaun and Wagner, 1985; Kasuya and Naeser, 1988; Tagami *et al.*, 1996, 1998; Yamada *et al*., 1995, 2003, 2007; Tagami and Shimada, 1996; Rahn, 2001; Garver, 2003; Hasebe *et al*., 2003; Rahn *et al*., 2004; Reiners and Brandon, 2006). The PAZ varies with the composition, the orientation of the crystals, and the metamictization degree in the case of zircons (Carlson *et al*., 1999; Green *et al.*, 1986; Ketcham *et al.*, 1999, 2007).

In this study, ten samples were analyzed by low temperature thermochronology. Among them, eight samples were analyzed for ZFT and six for AFT (Table 1). The samples correspond to different Silurian to Permian lithostratigraphic units and come from outcrops in the Ventana Ranges and from an exploration well drilled in the Claromecó Basin (PANG 003 well, see location in Fig. 2).

The samples were processed, measured and modeled in the Thermochronology Laboratory La.Te. Andes (Salta, Argentina). The minerals were separated by crushing, grinding, heavy liquids and magnetic methods; they were mounted and polished and the tracks were revealed by etching. The prepared samples were irradiated in the RA3 reactor located in the CNEA facilities in Ezeiza (Argentina), to generate induced tracks. The measurements were done with a binocular microscope Zeiss® AXIO Imager Z2m and Software TrackWorks® Autoscan®. The ages were calculated by the external detector method (ζ value) (Huford and Green, 1981, 1982, 1983; Wagner Van den Haute, 1992), and the data processed with TrackKey© Software (Dunkl, 2002).

All data were integrated in numerical models using the HeFTy 1.9.3 software (Ketcham, 2017). This was possible in the samples with a larger quantity of measured confined tracks. The aim of this work was to model cooling/heating paths statistically reliable using the "Good Fit" method (Goodness of Fit > 50%), obtaining the "Best Fit" path, with inverse modeling. Sample location, elevation and depth, stratigraphy and thickness are important in the modelling. The thermochronological data (ages per grain, D-par and length of confined tracks) were also integrated with previous data as U-Pb ages, vitrinite reflectance and fluid inclusions temperatures, provenance, paleomagnetism data and anisotropy of magnetic susceptibility (Arzadún *et al*., 2013, 2017). This integration allowed us to calibrate the interpretation of the time-temperature evolution of the study area.

Table 1. Sample information, with the stratigraphic unit, ages, lithology and area of situation, coordinates (WGS 84) and elevation or depth (in negative numbers).

Sample	Stratigraphic unit	Lithology	Area	Stratigraphic age (Ma)	Coordinates		Elevation/ depth (m)	Analysis
					X	Y		
SVN034	Napostá Fm	Quartz-rich sandstone	Ventana Ranges	Silurian (440-420)	587507.17 m E	5785211.78 m S	539	ZFT
12VL 09	Lolén Fm	Sandstone	Ventana Ranges	Devonian (420-360)	596932.51 m E	5773989.08 m S	442	AFT ZFT
SVL 039	Lolén Fm	Sandstone	Ventana Ranges	Devonian (420-360)	593241.23 m E	5786751.11 m S	384	AFT ZFT
SVL 061	Lolén Fm	Sandstone	Ventana Ranges	Devonian (420-360)	603486.77 m E	5775785.56 m S	291	AFT ZFT
SVSG1/17	Sauce Grande Fm	Sandstone	Ventana Ranges	Devonian (360-300)	598712.47 m E	5786122.57 m S	363	AFT ZFT
R76	Tunas Fm	Tuff	Ventana Ranges	Permian (U/Pb: 291 Ma) (Arzadún *et al.*, 2018)	600135.00 m E	5805887.00 m S	400	ZFT
R51	Tunas Fm	Tuff	Ventana Ranges	Permian (U/Pb : 284-280 Ma) (Tohver *et al.*, 2008; López Gamundi *et al.*, 2013; Alessandretti *et al.*, 2013)	632727.00 m E	5769414.00 m S	410	AFT
P811	Tunas Fm	Tuffaceous sandstone	PANG0003 well Claromecó Basin	Permian (U/Pb: 294-289 Ma) (Arzadún *et al.*, 2018)	647285.46 m E	5841392.52 m S	-811	AFT ZFT
P608	Tunas Fm	Tuffaceous sandstone	PANG0003 well Claromecó Basin	Permian	647285.46 m E	5841392.52 m S	-608	ZFT
P489	Tunas Fm	Tuffaceous sandstone	PANG0003 well Claromecó Basin	Permian	647285.46 m E	5841392.52 m S	-489	ZFT

4. Results

a. Data

In order to have a good representation of the Paleozoic column, 10 samples were collected, well distributed in the stratigraphic succession of the study area (Fig. 4). However, some of the samples were not suitable for AFT and ZFT analysis, due to the absence or bad quality of the mineral grains (Table 1). Seven of the analyzed samples were obtained from outcrops in the Ventana Ranges: one quartzite from Napostá Fm (Silurian) that was suitable only for ZFT, three sandstones from the Lolén Fm (Devonian), one sandstone from the Carboniferous Sauce Grande Fm, and two tuff from the Tunas Fm (Permian) (Table 1), one of them suitable for ZFT and the other one for AFT. In addition, three samples were recovered from the PANG 0003 well cores, situated at the Claromecó Basin, corresponding to tuffaceous sandstones from the Tunas Fm, two of them suitable only for ZFT (Table 1).

The PANG 003 well penetrated 191 m of Cenozoic sediments and more than 700 m of sedimentary rocks of the Tunas Formation (Early Permian). This sequence is represented by medium-to-fine-grained sandstones interbedded with mudrocks, thin tuffaceous levels, carbonaceous mudrocks and coal beds (Arzadún *et al.*, 2018, see Fig. 4B).

The detailed results of AFT ages and the kinetic parameters of Dpar and confined length of traces (corrected by a crystallographic orientation by the software HeFTy©) are presented in Table 2. All analyzed samples have a unique statistic population, meaning they display total annealing (i.e. they reached at least 60-120°C during 10 My), so the obtained ages are considered as cooling ages. The samples from the Lolén and Sauce Grande formations (Devonian and Carboniferous respectively) present cooling ages corresponding to the Late Jurassic (samples 12VL09, SVL061, SVL039 and SVSG1/17; Figs. 4A, 4B, 4C and 4D). Results of Tunas Formation (Permian) yield Early Jurassic cooling ages in the outcrop sample from the Ventana Ranges (sample R51; Fig. 4E); while in the sub-surface of the Claromecó Basin, this unit yielded an Early Cretaceous cooling age (sample P811; Fig. 4F).

The detailed results of ZFT analyses are presented in Table 3. Among the samples take, the one from the Napostá Fm (Silurian, sample SVN034) has a unique statistic population, with total annealing (meaning it reached at least 200-300° C during 10 My); thus the obtained Early Jurassic ages are considered as cooling ages (Fig. 5A). In addition, one sample from the Devonian Lolén Fm 12VL 09) and the sample of the Carboniferous Sauce Grande Fm (SVSG1/17) have a unique statistic population (also interpreted as due to total annealing). The sample from the Lolén Fm (12VL09) displays an Early Jurassic cooling age (Fig. 4B), while the sample from the Sauce Grande Fm (SVSG1/17) yielded a Late Triassic-Early Jurassic cooling age (Fig. 5E). The other two samples from the Devonian Lolén Fm (SVL061 and SVL039) display ages populations that indicate partial

annealing (Figs. 5C and 5D). The Permian samples from the Tunas Fm show the same behavior (P811, P607 and P489; Figs. 5F, 5G and 5H).

Table 2: AFT data. Central age calculated with IRMM 540 dosimetric glasses and z-calibration = 341.6 ± 21.8 Ma. N: number of grains measured. ρ_s: density of spontaneous fission tracks (x 10^5 cm^{-2}). Ns: total number of spontaneous fission tracks. ρi and ρd: density of induced fission tracks and the dosimeter(x 10^6 cm-2), calculated with N= 5000, in the external detector (g=0.5). Ni: total number of induced fission tracks in the sample. P(χ2): probability to obtain a χ2 value for n degrees of freedom (n= cristal number -1), samples with probability >5% are indicative of a homogeneous population. Average length and number (N) of confined fission tracks. Average and number (N) Dpar.

Sample	Stratigraphic age	N	U (ppm)	Dosimeter (ρD)	Spontaneous		Induced		P $(X)^2$ %	Age disp.	Central age (Ma) ± 1s	Confined		Dpar	
					ρ_S	N_S	ρ_I	N_I				N	Length av. (µm)	N	Av. (µm)
12VL 09	Devonian	34	31.6	11.9	19.2	1873	25.2	2459	15.0	0.09	**158.7 ± 11.5**	45	**13.8**	176	**1.5**
SVL 061	Devonian	28	55.8	12	10.0	744	14.4	1065	55.8	0.02	**146.5 ± 11.6**	7	**14.2**	141	**1.5**
SVL 039	Devonian	34	17.8	12.1	12.2	1788	15.9	2324	59.3	0.07	**164.6 ± 11.9**	60	**13.9**	176	**1.6**
SVSG1/17	Carboniferous	30	31.6	11.7	18.0	1086	24.9	1501	16.8	0.11	**149.8 ± 11.8**	35	**13.5**	154	**1.5**
R51	Permian	30	11.9	12.3	8.8	353	9.9	400	98.1	0.01	**188.5 ± 18.2**	3	**14.6**	169	**1.9**
P811	Permian	34	19.8	12.5	9.0	524	15.8	916	68.2	0.05	**125.8 ± 10.6**	18	**13.3**	132	**1.8**

Tabla 3: ZFT data. Central ages calculated with IRMM 541 dosimetric glasses and z-calibration = 120.89 ± 4.73 Ma and 122.48 ± 4.89 Ma (for samples P608 and P489). N: number of measured grains. ρ_s: spontaneous fission track density (x 10^5 cm^{-2}). Ns: total number of spontaneous fission tracks. ρi and ρd: induced fission track density in the samples and the dosimeter, calculated with N= 5000, in the external detector (x 106 cm-2) (g=0.5). Ni: total number of induced fission tracks in the sample. $P(\chi)^2$: probability to obtain a χ^2 value for n degrees of freedom (n= number of crystals -1), samples with probability >5% are indicative of a homogeneous population, while <5% are analyzed with the binomial peak adjustment method, P1, P2 and P3 are the population ages obtained from the Binomfit software, with its error (± 1s) and percentage (%).

Sample	Stratigraphic age	N	U (ppm)	Dosimeter (ρD)	Spontaneous		Induced		P $(X)^2$ %	Age disp.	Central age (Ma) ± 1s	P1 ± 1s (%)	P2 ± 1s (%)	P3 ± 1s (%)
					ρ_S	N_S	ρ_I	N_I						
SVN 034	Silurian	26	185.6	5.2	137.5	2644	23.0	443	63.9	0.03	**184.8 ± 12.3**	-	-	-
12VL 09	Devonian	29	188.5	5.2	148.2	4704	23.2	736	86.4	0.01	**198.6 ± 11.4**	-	-	-
SVL 061	Devonian	44	155.3	5.18	154.1	9718	17.7	1119	4.5	0.13	**265.6 ± 15.0**	**248.9 ± 17.2 (79.2)**	**352.5 ± 55.7 (20.8)**	-
SVL 039	Devonian	33	249.4	5.16	235.1	9794	31.7	1328	0.0	0.30	**327.6 ± 16.8**	**182.4 ± 14.2 (52.7)**	**260.9 ± 38.6 (28.7)**	**457.4 ± 35.8 (18.6)**
SVSG1/17	Carboniferous	29	227.9	5.24	176.7	5627	27.4	873	12.5	0.11	**201.5 ± 11.9**	-	-	-
R76	Permian	27	192.9	5.29	204.5	3853	24.0	453	0.24	0.25	**233.2 ± 18.4**	**267.4 ± 22.4 (77.5)**	**155.0 ± 28.05 (22.5)**	-
P811	Permian	35	298.9	5.11	298.1	7317	37.7	926	0.66	0.17	**236.6 ± 14.7**	**262.6 ± 17.8 (73.7)**	**181.7 ± 22.8 (26.3)**	-
P 608	Permian	35	163.9	5.18	148.2	6282	19.2	813	1.5	0.16	**240.6 ± 15.2**	**260.0 ± 18.8 (83.9)**	**170.5 ± 35.7 (16.1)**	-

P 489	Permian	30	140.8	5.16	129.7	4768	18.1	664	0.03	0.23	**213.8 ± 15.8**	**254.7 ± 17.1 (73.0)**	**142.6 ± 15.9 (27.0)**	-

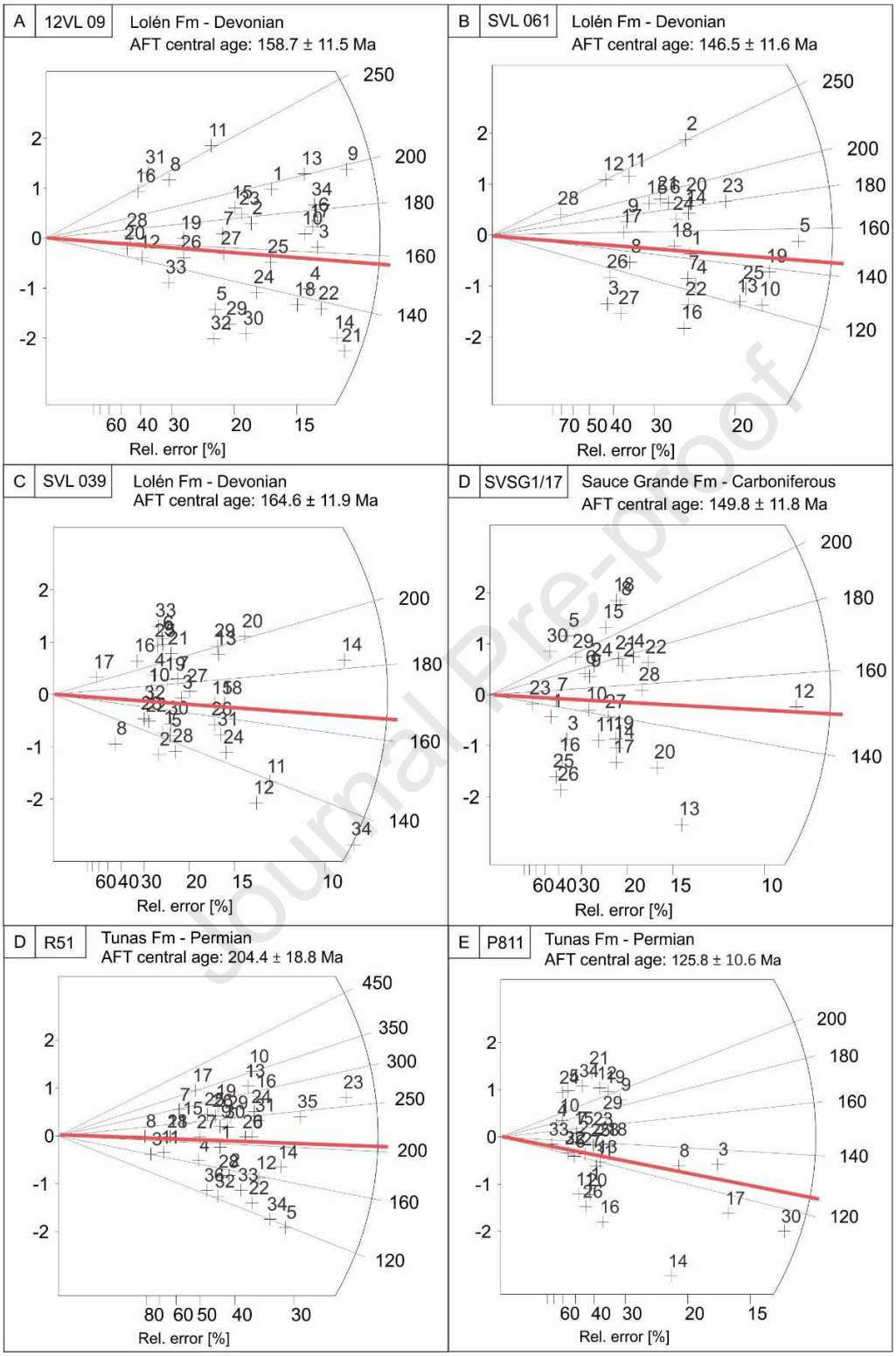

Figure 4. Radial distribution of the AFT ages of the different samples, central age is in red.

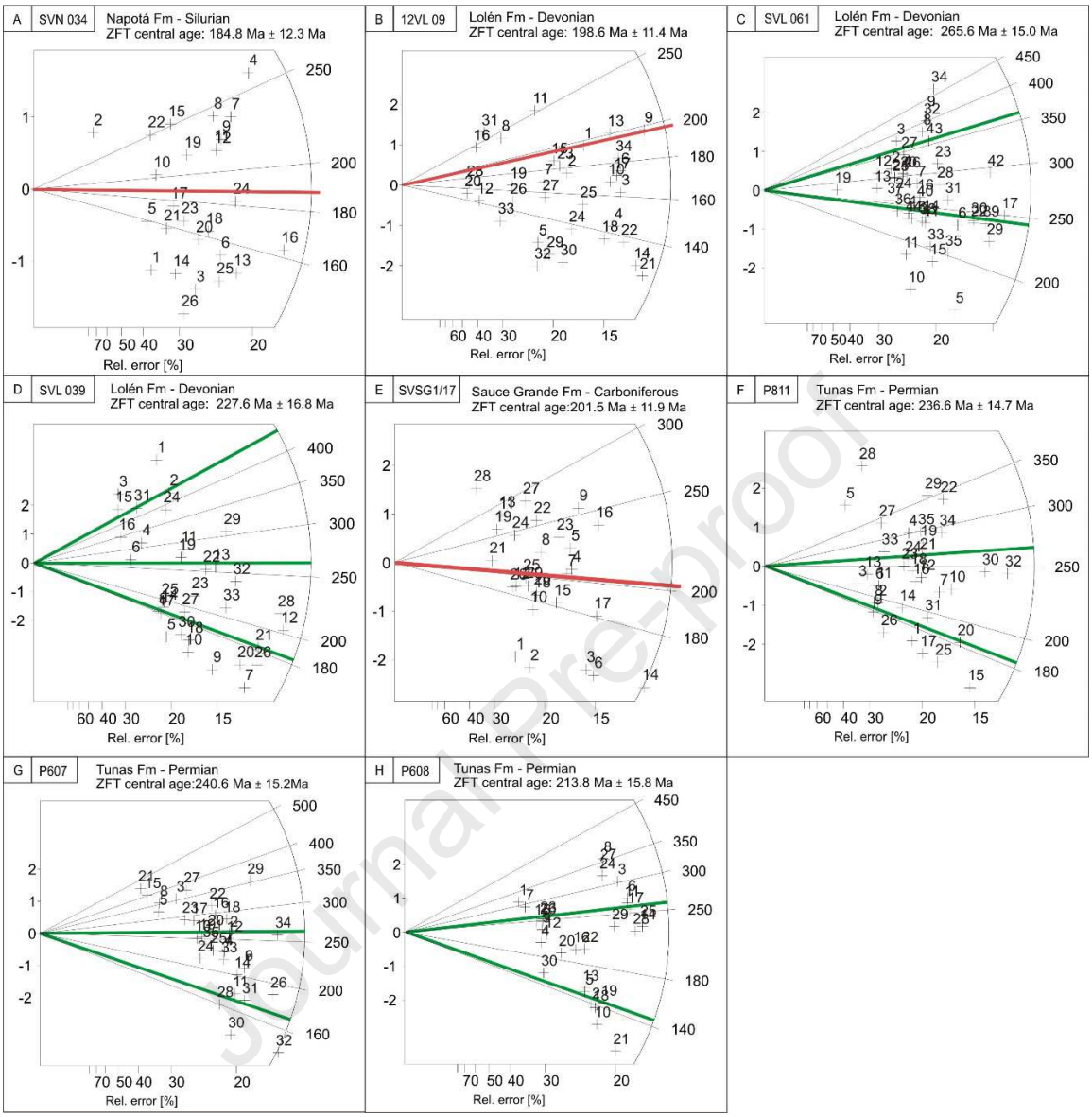

Figure 5. Radial distribution of the ZFT ages of the different samples, central age is in red and in green are the ZFT population ages.

b. Kinetic parameters (Dpar and length)

The Dpar is a useful parameter to qualitatively approximate the chemical composition of the apatite grains, regarding the chlorine and fluorine content that is related to the annealing temperature of the fission tracks. Larger Dpar values indicate higher concentrations of chlorine and higher temperature values.

In each sample, the distribution of the Dpar and the fission track lengths were analyzed in relation to lithostratigraphic unit ages. All samples have similar length of confined tracks, between 13.3 and 14.6 µm, and there are no important differences in the

Dpar values of each sample. However, there are differences in the Dpar values between formations, e.g. the Lolén and the Sauce Grande Formations (Devonian and Carboniferous respectively) have values between 1.5 and 1.6 µm, while the Tunas Formation (Permian) displays higher values between 1.8 and 1.9 µm (Fig. 6). These values indicate a different composition with respect to the other units, so a different sediment provenance, and a larger resistance to annealing.

Regarding the length of the confined tracks, there are no important differences in values, which are between 13 and 14.6 µm (Table 2). These lengths show that there is no shortening of the tracks and confirm the AFT total annealing. In the Lolén, Sauce Grande and Tunas samples with enough data, the measured lengths display a unimodal and geometric distribution. The samples with larger quantity of length data were used in modelling.

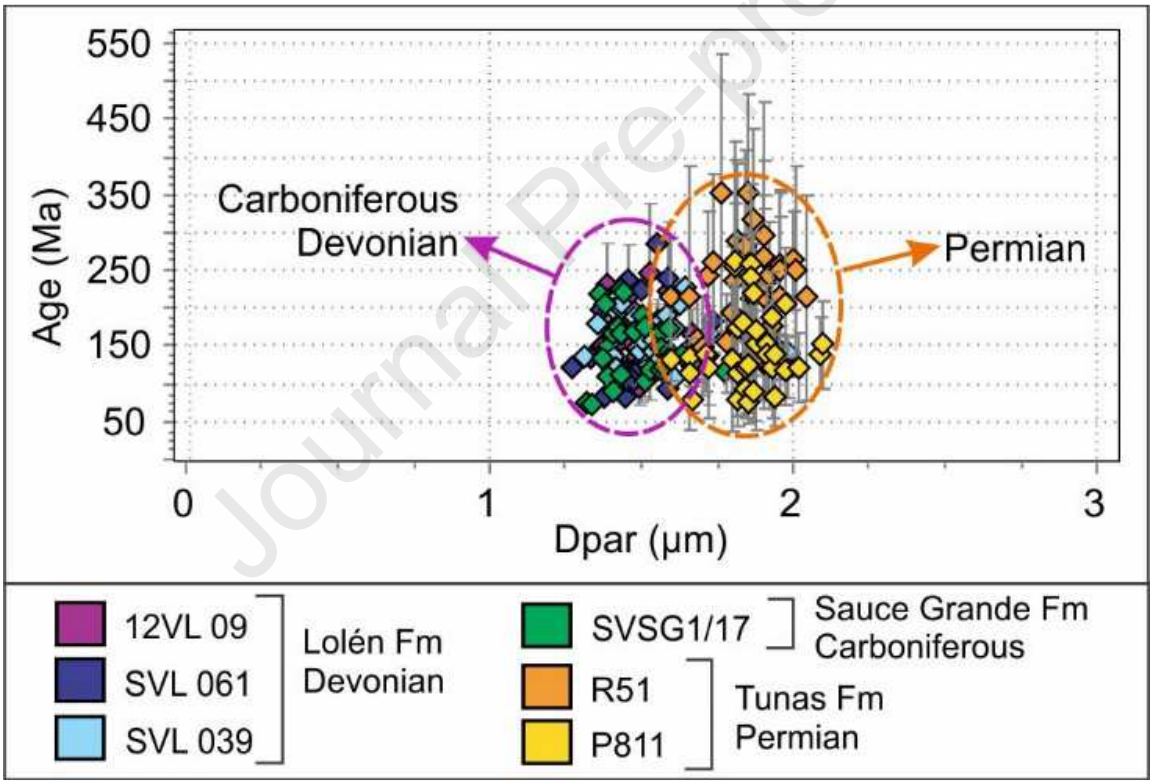

Figure 6. Ratio between the Dpar parameter and fission track age in the different samples that clearly show the existence of two different population in the data.

c. Time-Temperature Numerical Models

Three samples were modelled with the Hefty software, one of them from outcrops of the Lolén Fm (Devonian, SVL039), one from outcrops of the Sauce Grande Fm (Carboniferous, SVSG17/1), and one from the Tunas Fm (Permian, P811) recovered from

the PANG003 well. it was possible to get a number of models with a good a fit (GOF>50%) for all three samples.

To produce the models, the ZFT and AFT ages were used when avaliable, with its respective Dpar and length data. Also, the present altitude (or depth) of the samples was considered together with the stratigraphic age (using geochronological data when available). To validate the models, they were integrated with the tectonic and stratigraphic evolution, considering the thicknesses of the different formations and existing temperature data. Using all these elements is very important in the construction of coherent time-temperature paths. The measured thicknesses were translated to a time-temperature space crossplot, using a normal geothermal gradient of 30°C/km.

Geochronological data used to calibrate the age of the Tunas Fm come from interbedded tuff levels cropping out in the Pillahuincó Range: a U/Pb zircon age of 291 Ma (Arzadún *et al.*, 2018), U/Pb zircon ages of 280 and 284 Ma (Tohver *et al.*, 2008; López Gamundi *et al.*, 2013; Alessandretti *et al.*, 2013), and two new LA-ICP-MS U–Pb zircon ages of tuff levels from the Las Mostazas quarry than suggest that the deposits are younger than 286 Ma (Ballivián Justiniano *et al*., 2020). Particularly in well PANG003, U/Pb zircon ages of 289 and 294 Ma were obtained by Arzadún *et al.* (2018) for tuff levels at 800 m MD (measured depth).

Regarding other temperature data, minimum temperatures of 140 and 160°C were obtained from fluid inclusion analysis thermometry data in outcrop and subsurface samples of the Tunas Fm (Arzadún *et al.*, 2013), and a maximum temperature of 190°C was obtained from vitrinite reflectance in the PANG003 well at 842 m MD (Arzadún *et al.*, 2017).

Moreover, the model also incorporates the tectonic evolution of the study area. Paleomagnetic data indicate two different pole positions during the Permian, at 291 and 281 Ma, supporting the syn-tectonic deposition of this unit (Tomezzoli and Vilas, 1999; Tomezzoli, 2001; Arzadún *et al.*, 2018). Petrographic data indicate a change in provenance during Permian (Andreis and Cladera, 1992; López Gamundi, 1996), which is validated by the detrital zircon content (Ramos *et al*., 2013). Anisotropy of magnetic susceptibility data (Arzadún *et al.*, 2017), structural data (Tomezzoli and Cristallini, 1998), re-crystallization age of illite (Buggish, 1987), and the presence of growth strata (López Gamundi *et al.*, 1995) indicate active deformation event during the Permian in the Ventana Ranges, with compressive stress from the southwest (Gondwanide orogeny), and decreasing towards the foreland Claromecó Basin.

All the previously mentioned data were combined to analyze the possible time-temperature paths and to fit the model and interpretations on the evolution of the basin (Fig. 7).

Sample SVL 039 (Fig. 7A) is a sandstone from the Devonian Lolén Fm. As the ZFT does not show total annealing, we interpret that the sample was not exposed to a temperature above 200-300° C. Only AFT data were used for the modeling. The AFT central age (164.6 ± 11.9 Ma) was tested against the geological constrains. 60 length

measures were obtained in this sample and were used to calibrate the model. 10,000 statistic iterations were carried out and 217 time-temperature acceptable paths were obtained, with 5 good paths with good fit (GOF) (Fig. 7A).

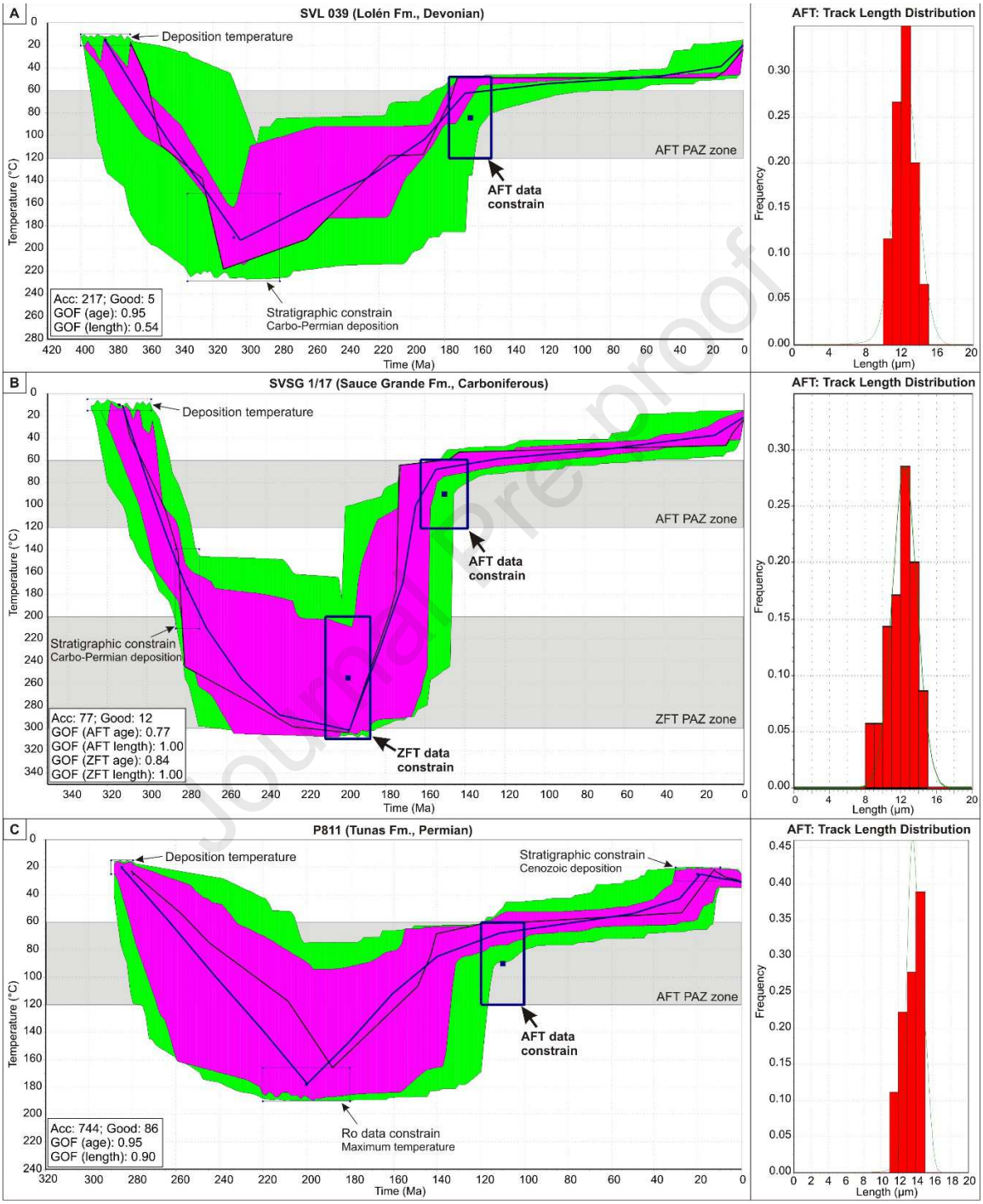

Figure 7. Time-Temperature numerical models obtained by HeFTy software (Ketcham, 2005; Ketcham, 2011; Ketcham *et al*., 2007a, b; Ketcham *et al*., 2009). Different constrains were used: stratigraphy, considering the thickness of the deposits above the sample (geothermal gradient = 30°C/km), temperatures reached by the Permian deposits (from R_0 and fluid inclusion data), and AFT-ZFT data. The results show three different reliability levels; green: acceptable adjust (all paths with Goodness of Fit (GOF) > 0.05 (5%)),

pink: good adjust (all paths with GOF > 0.5 (50%), black line: t-T path of best fit, blue line: weighted average path. Acc: number of acceptable fit models. GOF: number of good fit models. In gray, PAZ zones. **A.** Sample SVL 039 from the Devonian Lolén Formation. **B.** Sample SVSG 1/17 from the Carboniferous Sauce Grande Formation. **C.** Sample P811 from the Permian Tunas Formation in subsurface.

Sample SVSG1/17 (Fig. 7B) corresponds to a sandstone from the Carboniferous Sauce Grande Fm. An AFT central age of 149.8 ± 11.8 Ma and a ZFT central age of 201.5 ± 11.9 Ma were tested with the geological constrains. 35 length measures were obtained from this sample. 10,000 statistic iterations were performed and 77 time-temperature acceptable paths were obtained, with 12 good paths with good fit (GOF) (Fig. 7B).

Sample P811 is a sandstone from the Early Permian Tunas Fm, recovered from 811 m MD in the PANG003 well. The age of this succession is estimated between 294 and 289 Ma by extrapolation of the U/Pb ages obtained from interbedded tuff levels (Azardún *et al*., 2018). An AFT central age of 125.8 ± 10.6 Ma was tested with the geological constrain. No acceptable models could be obtained with the ZFT data, which is probably due to incomplete ZFT annealing. As such the sample was never exposed to temperatures above 200-300°C, which is in agreement with the vitrinite data. The sample has 18 measured lengths, and it was probe with 10,000 statistic iterations. 744 time-temperature acceptable paths were obtained, of which 86 good paths with good fit (GOF) (Fig. 7C).

The three models were constrained with the stratigraphy, assuming that the maximum temperatures were reached by Permian times and taking into account the thickness of the overlaying formations.

5. Discussion

The samples analyzed in the Ventana Ranges and the Claromecó Basin, display total annealing by AFT data. As such, the AFT ages are considered as cooling ages and therefore the samples reached temperatures of between 60 to 120°C or more for at least 10 My. The obtained data and the results of modeling agree with the temperature previously estimated from fluid inclusions microthermometry and vitrinite reflectance, of between 140° C and 190° C for Tunas Fm (Arzadún *et al*., 2013). These minimum temperatures are also consistent with green-schist metamorphic grade of the Devonian and Carboniferous units in the Ventana Ranges reported by Von Gosen *et al.* (1991).

According to the AFT data, the cooling/exhumation history of Silurian and Permian the units exposed along the Ventana Ranges show exhumation since the Late Triassic - Early Jurassic. This cooling event is recorded in the Permian units (sample R51, Tunas Fm, cooling age of 204.4 ± 18.8 Ma) at first, then in the Carboniferous and Devonian units (samples 12VL 09, SVL 061, SVL 039 from the Lolén Fm and SVSG 1/17 from Sauce Grande Fm) with cooling ages between 164.6 ± 11.6 Ma and 146.5 ± 11.6 Ma (Fig. 8).

In the Claromecó Basin, the samples obtained from different depths within the Permian Tunas Fm in the PANG003 well give very consistent results, and the AFT data

indicate younger cooling ages (Early Cretaceous, 125.8 ± 10.6 Ma) in sub-surface (basin) than in the Ventana Ranges (Fig. 8).

The ZFT data show clearly a total annealing in the sample from the Silurian Napostá Fm (SVN 034), indicating that this unit reached 200-300° C. A cooling event starting in the Early Jurassic is in agreement with the preserved stratigraphic thickness deposited above this unit. Sample SVSG 1/17 from the Carboniferous Sauce Grande Fm and sample 12VL 09 from the Devonian Lolén Fm display total annealing with similar cooling ages indicating exhumation in the Early Jurassic. The other samples from the Devonian series display partial annealing (samples SVL061 and SVL039) (Fig. 8). These could indicate that they were part of different blocks (as previously suggested by Cobbold et *al.*, 1987; Fig. 2). ZFT data of the samples from Permian units also indicate partial annealing, meaning these samples did not reach temperatures of 200-300°C for more than 10 My. In the samples with partial annealing, population ages were obtained, and the younger population ages are concordant with the cooling ages of the other samples (Fig. 8).

The thickness of the Devonian, Carboniferous and Permian units are insufficient to explain the temperatures obtained from the different methods, but are in agreement with previous data and, considering the major unconformity described in the succession, between the Early Permian Tunas Fm and the Cenozoic sediments, it seems reasonable that at least 2,000 m of additional column (considering a normal geothermal gradient) were eroded from the present-day top of the Tunas Fm in the subsurface of the Claromecó basin.

The exhumation of the Paleozoic series was cumulative throughout the Mesozoic and we interpret it, considering the location of the studied units with regards to the Mesozoic Colorado basin, as uplift occurring in the basin flank. In the Colorado Basin there are apatite fission track results in different units.

The AFT and ZFT ages obtained in this work are in agreement with AFT and zircon He (ZHe) previous ages obtained by Kollenz *et al.* (2016). As such, apatite He ages (AHe) obtained in the Permian Tunas Formation are between 120 Ma and 107 Ma (Early Cretaceous) (Fig. 9). The closing temperature of the AHe system is between 60-40°C, which supports the culmination of the third rifting stage culminated during the Early Cretaceous (Fig. 9).

Although there are no important differences in the length values of the confined tracks in the samples, the Dpar show similar values in the Lolén and Sauce Grande formations and larger values in the samples from the Tunas Formation (Fig. 6). These data evidence larger Chlorine content in the Permian grains and so different composition, in agreement with the petrographic analyses carried out by López Gamundi (1995) that indicate a change of provenance during the Permian.

The obtained thermochronology data in the Ventana Ranges are interpreted as produced by a long-lived exhumation event throughout the Mesozoic. The ZFT cooling ages of the Silurian, Devonian and Carboniferous units, and the AFT age of the Early Permian Tunas Fm, indicates a cooling event during the Late Triassic to Early Jurassic that is associated with the first and second rifting stages described by Lovecchio *et al.* (2018,

2020). This exhumation can be interpreted as rift flank exhumation (Fig. 9). The AFT ages of Tunas Fm in the Claromecó Basin indicate a cooling event during the Early Cretaceous that is interpreted as part of passive margin exhumation during the drift stage after the South Atlantic Ocean opening in the Early Cretaceous (third rifting stage) (Fig. 9). The AHe ages obtained by Kollenz *et al.* (2016) in the outcrops of Tunas Fm, allow extending the last rifting stage to 107-120 Ma (Lower Cretaceous).

The association of the cooling ages with the different rifting events and the eroded thickness of at least 2000 m, confirm that the Ventana Ranges-Claromecó Basin acted as part of the northern flank of the Colorado Basin during its Mesozoic rifting history.

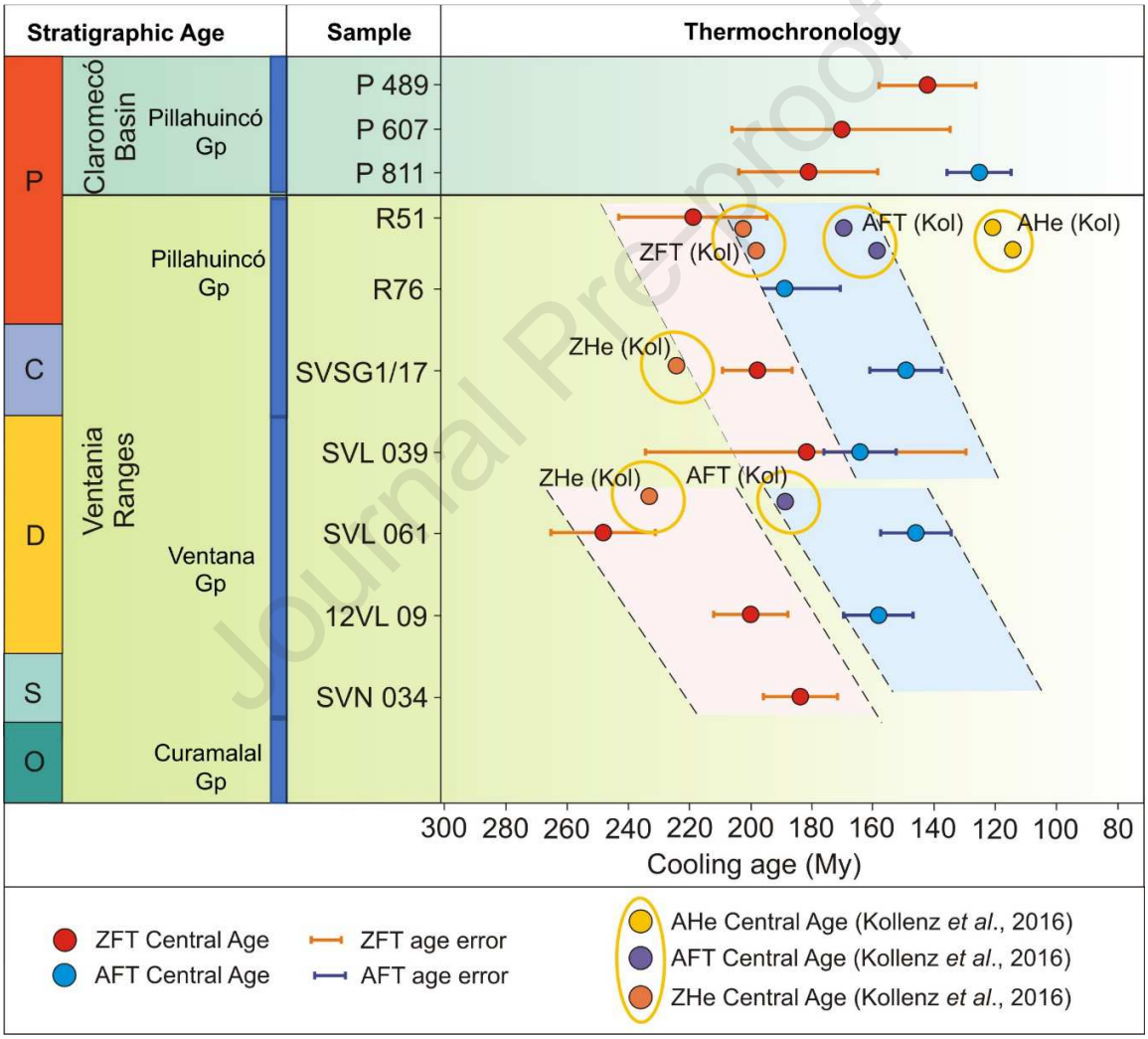

Figure 8. AFT (blue spots) and ZFT (red spots) cooling ages in samples from Ventana Ranges and Claromecó Basin, with its associated errors. Sedimentary units and their corresponding ages are plotted along the vertical axis. Cooling ages from thermochronology (central age and associated error bars) are plotted along the horizontal axis. Pink and light blue dashed areas follow a logical cooling sequence. Comparison with Kollenz *et al*. (2016): AFT data, (U-Th-Sm)/He in apatite (AHe) and in zircon (ZHe).

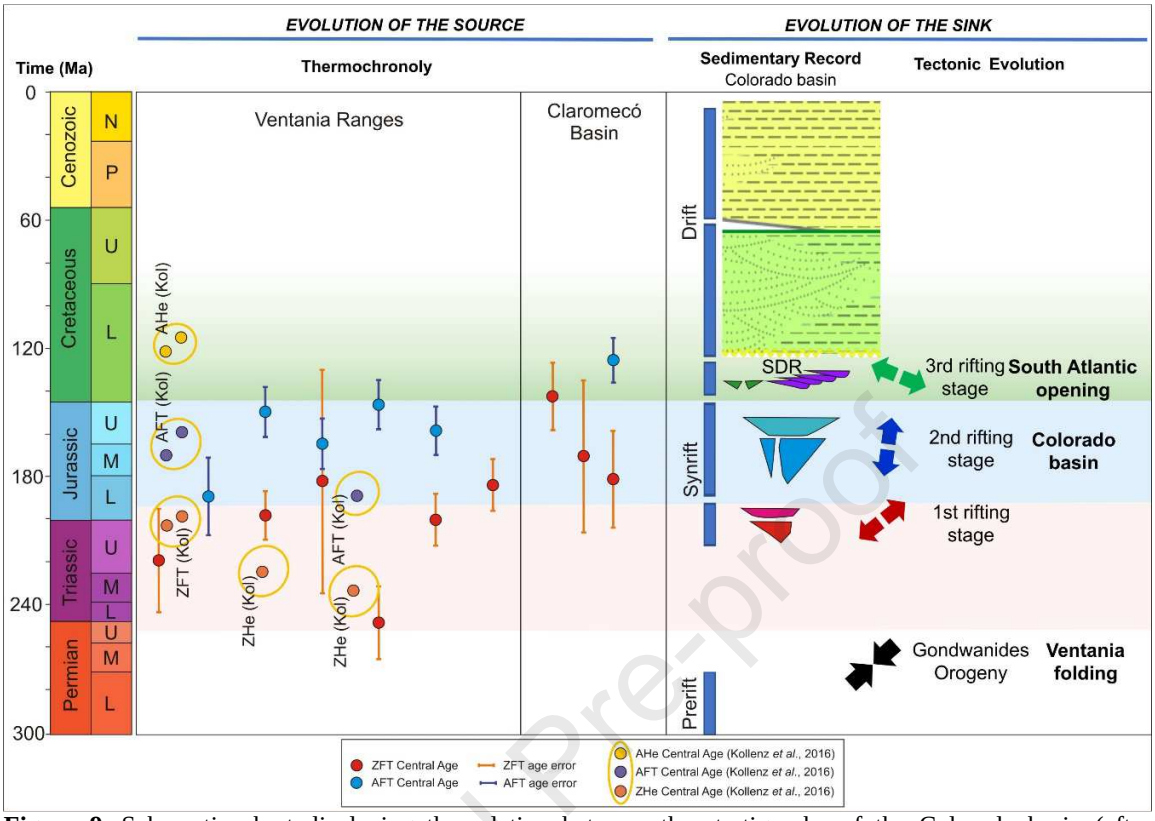

Figure 9. Schematic chart displaying the relation between the stratigraphy of the Colorado basin (after Lovecchio *et al*., 2018) and the thermochronology data both from the new samples herein presented (AFT and ZFT from the Ventana Ranges and Claromecó Basin) and the data from Kollenz et al (2016) (AFT, AHe, ZHe). Ages are plotted on the vertical axis. The chart highlights synchronicity between rifting in the Colorado Basin and exhumation (uplift) of the Ventana Ranges and Claromecó Basin both along the northern flank of the basin. Sampled units are shown on Fig. 8.

6. Conclusions

The Ventana Ranges and its associated Claromecó foreland basin, form a system that records a complex tectono-stratigraphic evolution, with onset of a passive margin in the early Paleozoic, later on affected by a major Gondwanan glaciation in the late Paleozoic and compressive tectonic events and foreland sedimentation in the early Permian.

The thermochronology study presented here and the obtained cooling ages for the Ventana Ranges are interpreted as a long-lived, probably multi-stage, exhumation event occurred throughout the Mesozoic. The ZFT ages indicate that the Silurian, Devonian and Carboniferous units cooled from the ZFT PAZ (partial annealing zone between 200 and 300°C) during the Late Triassic to Early Jurassic. The AFT age of the Early Permian Tunas Fm, indicates a cooling event from the AFT PAZ (partial annealing zone between 60 and 120°C) also during the Early Jurassic. These ages are consistent with the first rifting stage described by Lovecchio *et al.* (2018, 2020), where this exhumation stands for rift flank uplift (Fig. 9). The Late Jurassic cooling AFT ages obtained from the Devonian and

Carboniferous formations could indicate that these units were exhumed during the second and third rifting stages described by Lovecchio *et al.* (2018, 2020).

In the Claromecó Basin, the AFT ages of Tunas Fm, indicate a cooling event from the AFT PAZ (partial annealing zone between 60 and 120°C) during the Early Cretaceous, interpreted as part of passive margin exhumation during the drift stage after the South Atlantic Ocean opening in the Early Cretaceous (third rifting stage) (Fig. 9). In addition, The AHe ages obtained by Kollenz *et al.* (2016) for the Ventana Ranges record this same event (Fig. 9).

The thermochronological data presented here and the time-temperature numerical models show that most of the exhumation in the study area was accomplished during the Mesozoic and that a thickness of at least 2,000 m of Permian must have been eroded from the top of the Tunas Fm to have produced total annealing for ZFT and AFT for the Devonian, Carboniferous and Permian samples in the Ventana Ranges, and for the Permian samples collected from the Claromecó basin.

Acknowledgments

This work was supported by YPF S.A. (Argentina).We are grateful to YPF S.A. and LA.TE. ANDES for their permission to publish the data here included. We would like to thank LA.TE. ANDES Productive and Research Center (GEOMAP-CONICET, Salta Province, Argentina) for the contributions made in the application of thermochronology. We also thanks to Universidad Nacional del Sur and Universidad Nacional de La Plata for providing some of the samples, and special thanks to Prof. Dr. Ulrich Glasmacher for the contribution of knowledge and data review. Special thanks to reviewers Renata N. Tomezzoli and Cecilia del Papa for their contributions and comments that improved this paper.

References

Amos, A.J. and Urien, C.M., 1968. La falla "Abra de la Ventana" en las Sierras Australes de la provincia de Buenos Aires. Revista de la Asociación Geológica Argentina, 23 (3): 197-206.

Andreis, R.R. 1984. Análisis litofacial de la Formación Sauce Grande (Carbónico superior?), Sierras Australes, provincia de Buenos Aires. Anual Meeting Project 211-IGCP, “Late Paleozoic of South America”, San Carlos de Bariloche, Río Negro, pp. 28- 29.

Andreis, R.R. and Japas, S., 1996. Cuencas Sauce Grande y Colorado. En: S. Archangelsy (Ed.), El Sistema Pérmico en la República Argentina y en la República Oriental del Uruguay. Academia Nacional de Ciencias, 45-64.

Andreis, R.R. and Cladera, G., 1992. Las epiclastitas pérmicas de la Cuenca Sauce Grande (Sierras Australes, Buenos Aires, Argentina). Parte 1: Composición y procedencia de los detritos. Actas 4º Reunión de Sedimentología, 1: 127-134.

Andreis, R.R., Lluch, J.J. and Iñiguez Rodríguez, A.M., 1979. Paleocorrientes y paleoambientes de las Formaciones Bonete y Tunas, Sierras Australes de la Provincia de Buenos Aires, Argentina. Actas 6° Congreso Geológico Argentino, Buenos Aires. 2: 207-224.

Andreis, R.R., Iñiguez Rodríguez, A.M., Lluch, J.J. and Rodríguez, S., 1989. Cuenca paleozoica de ventania. Sierras Australes de la provincia de Buenos Aires. En: Chebli, G. Spalletti, L. (Eds.): Cuencas sedimentarias argentinas. Serie Correlación Geológica, 6:265-298.

Alessandretti, L., Philipp, R.P., Chemale, F., Brückmann, M.P., Zvirtes, G., Metté, V. and Ramos, V.A., 2013. Provenance, volcanic record, and tectonic setting of the Paleozoic Ventania Fold Belt and the Claromecó Foreland Basin: implications on sedimentation and volcanism along the southwestern Gondwana margin. Journal of South American Earth Sciences. 71 pp.

Álvarez, G.T., 2004. Cuencas Paleozoicas asociadas a la prolongación norte del sistema de Sierras de Ventania, Provincia de Buenos Aires. PhD Tesis. Universidad Nacional del Sur. Argentina.

Archangelsky, S., Azcuy, C.L., González, C.R. and Sabattini, N., 1987. Correlación general de biozonas. En: S. Archangelsky (Ed.), El Sistema Carbonífero en la República Argentina. Academia Nacional de Ciencias, 281-292.

Archangelsky, S. and Cúneo, R., 1984. Zonación del Pérmico continental de Argentina sobre la base de sus plantas fósiles, 3º Congreso latinoamericano Paleontológico, México. Memoria, pp. 143-153.

Arzadún, G., Tomezzoli, R.N., Trindade, R., Gallo, L.C., Cesaretti, N.N. and Calvagno, J.M., 2018. Shrimp zircon geochronology constrains on Permian piroclastic levels, Claromecó Basin, southwest margin of Gondwana, Argentina. Journal of South American Earth Sciences. 85:191-208.

Arzadún, G., Cisternas, M.E., Cesaretti, N.N. and Tomezzoli, R.N. 2017. Presence of charcoal as evidence of paleofires in the Claromeco Basin, Permian of Gondwana, Argentina: Diagenetic and paleoenvironment analysis based on coalpetrography studies. GeoRes Journal.

Arzadún, G, Cesaretti, N.N, Fortunatti, N., Cisternas, M.E., 2013. Análisis de petrografía y fluorescencia de inclusiones fluidas en carbonato de matas algáceas de la Formación Tunas, Cuenca de Claromecó, Provincia de Buenos Aires, Argentina. XI MINMET. pp. 165-170. ISBN: 978-950-605-758-9.

Ballivián Justiniano, C.A., Comerio, M.A., Otero G., Sato A.M., Coturel E.P., Naipauer M., Basei M..A.S., 2020. Geochemical, palaeontological, and sedimentological approaches of a syn-orogenic clastic wedge: Implications for the provenance of the Permian (Cisuralian) Tunas Formation, Ventania System (Argentina), Journal of South American Earth Sciences. 104, 102836.

Burmistrov, S. (1971): Un ensayo geotectónico de las Sierras Australes de la Provincia de Buenos Aires. Actas de la Reunión sobre la geología de las Sierras Australes Bonaerenses, Bahía Blanca: 33-50.

Autin, J., Scheck-Wenderoth, M., Loegering, M.J., Anka, Z., Vallejo, E., Rodriguez, J.F., Dominguez, F., Marchal, D., Reichert, C., di Primio, R. and Götze, H.J., 2013. Colorado Basin 3D structure and evolution, Argentine passive margin. Tectonophysics 604, 264–279.

Buggisch, W. E., 1987. Stratigraphy and Very Low Grade Metamorphism of the Sierras Australes de la Provincia de Buenos Aires (Argentina) and Implications in Gondwana Correlation. Zbl. Geol. Paläont. Teil I (7/8): 819-837.

Carlson W.D., Donelick R.A. and Ketcham R.A., 1999. Variability of apatite fission-track annealing kinetics. I. Experimental results. Am. Mineral, 84:1213–23

Catuneanu, O., Wopfner, H., Eriksson, P.G., Cairncross, B., Rubidge, B.S., Smith, R.M.H. and Hancox, P.J., 2005, The Karoo basins of south-central Africa: Journal of African Earth Sciences, v. 43, p. 211–253

Coates, D.A., 1969. Stratigraphy and sedimentation of the Sauce Grande Formation, Sierra de la Ventana, southern Buenos Aires Province, Argentina: 1st Symposium on Geology and Paleontology of Gondwana, v. 2, p. 799-816.

Cobbold, P., Gapais, D. and Rossello, E., 1991. Partitioning of transpressive motions within a sigmoidal foldbelt: the Variscan Sierras Australes, Argentina. Journal of Structural Geology. 13, 743–758.

Cobbold, P.R., Massabie, A.C. and Rossello, E.A., 1987. Hercynian wrenching and thrusting in the Sierras Australes Foldbelt, Argentina. Hercynica, 2(2): 135-148.

D' Elia, L., Bilmes, A., Franzese, J.R., Veiga, G.D., Hernández, M. and Muravchik, M., 2015. Early evolution of the southern margin of the Neuquén Basin, Argentina: Tectono-stratigraphic implications for rift evolution and exploration of hydrocarbon plays. J. South Am. Earth Sci. 64: 42-57.

Dimieri, L.V. and Di Nardo, L., 1992. Estructuras en el abra de la Rivera, Sierras Australes de Buenos Aires. Séptima Reunión de Microtectónica, Actas 1: 27-34.

Dimieri, L.V. and Japas, M.S., 1986. Trazas fósiles distorsionadas como indicadoras de la deformación de la Formación Napostá, abras de la Ventana y del Hinojo, Sierras Australes de Buenos Aires. Tercera Reunión de Microtectónica, Actas 1: 32-39.

Di Pasquo, M., Martínez, M.A. and Freije, H., 2008. Primer registro palinológico de la Formación Sauce Grande (Pennsylvaniano-Cisuraliano) en las Sierras Australes, provincia de Buenos Aires, Argentina. Ameghiniana. V.45. Nro. 1.

Dunkl, I., 2002. Trackkey: a Windows program for calculation and graphical presentation of fission track data: Computers & Geosciences, v. 28, p. 3-12.

Dunkl, I., and Székely, B., 2002, Component analysis with visualization of fitting - Popshare, a Windows program for data analysis, Goldschmidt Conference Abstracts, Geochimica et Cosmochimica Acta 66 (15A), p. 201.

Du Toit A.L., 1927. A Geological Comparison of South America with South Africa. Carnegie Inst. Publ. N. 381, 157 p.

Fryklund, B., Marshall, A. and Stevens, J., 1996. Cuenca del Colorado. XIII Congreso Geológico Argentino y III Congreso de Exploración de Hidrocarburos. Geología y Recursos Naturales de la Plataforma Continental Argentina. Eds: V.A. Ramos y M.A. Turic. Relatorio 8: 135-158.

Frizon De Lamotte, D., Fourdan, B., Leleu, S., Leparmentier, F. and De Clarens, P., 2015. Style of rifting and the stages of Pangea breakup. Tectonics 34, 1009–1029.

Furque, G., 1973. Descripción geológica de la Hoja 34n, Sierra de Pillahuincó, Provincia de Buenos Aires. Boletín del Servicio Nacional de Minería y Geología, Buenos Aires, 141, 70 pp.

Garver, J.I., 2003. Etching zircon age standards for fission-track analysis. Radiation Measurements, 37(1): 47-53.

Gerster, R., Welsink, H., Ansa, A. and Raggio, F., 2011. Cuenca de Colorado. VIII Congr. Explor. y Desarro. Hidrocarburos Simp. Cuencas Argentinas visión actual 65–80.

Gleadow A. J. W. and Fitzgerald P. G., 1987. Uplift history and structure of the Transantarctic Mountains: new evidence from fission track dating of basement apatites in the Dry Valleys area, southern Victoria Land. Earth planet. Sci. Left. 82, 1-14.

Green, P.F., 1981, "Track-in-track" length measurements in annealed apatites: Nuclear Tracks, v. 5, p. 121-128.

Green, P.F., Duddy, I.R., Gleadow, A.J.W., Tingate, P.R. and Laslett, G.M., 1986. Thermal annealing of fission tracks in apatite, 1. A qualitative description. Chem. Geol. (Isot. Geosci. Sect.), 59: 237-253.

Green, P.F. and Durrani, S.A., 1977, Annealing studies of tracks in crystals: Nuclear Track Detection, v. 1, p. 33-39.

Gregori, D.A., Grecco, L.E. and Llambías, E.J., 2003. El intrusivo López Lecube: Evidencias de magmatismo alcalino Gondwánico en el sector sudoeste de la provincia de Buenos Aires, Argentina. Revista de la Asociación Geológica Argentina 58, 167–175.

Gregori, D.A., Kostadinoff, J., Strazzere, L. and Raniolo, A., 2008. Tectonic significance and consequences of the Gondwanide orogeny in northern Patagonia, Argentina. Gondwana Research, 14:429-450. Elsevier.

Hälbich, I., 1983. A tectogenesis of the Cape Fold Belt, in: Söhnge, A.P.G., Hälbich, I.W. (Eds.), Geodynamics of the Cape Fold Belt. The Geological Society of South Africa, Special Publication, 12, pp. 165–175.

Hansma, J., Tohver, E., Schrank, C., Jourdan, F. and Adams, D., 2016. The timing of the Cape Orogeny: New 40 Ar/ 39 Ar age constraints on deformation and cooling of the Cape Fold Belt, South Africa. Gondwana Research, 32: 122–137.

Harrington, H.J., 1947. Explicación de las Hojas Geológicas 33m y 34m, Sierras de Curamalal y de la Ventana, Provincia de Buenos Aires. Servicio Nacional de Minería y Geología, Boletín 61.

Harrington, H.J., 1972. Sierras Australes de Buenos Aires. En: A.F. Leanza (dir y ed.), Geología Regional Argentina. Academia Nacional de Ciencias, p.401.

Harrington, H.J., 1980. Sierras Australes de la Provincia de Buenos Aires. En: Turner, J.C.M., coord., Geología Regional Argentina 2: 967-983. Academia Nacional de Ciencias, Córdoba. (Reimpresión de Harrington, 1972a).

Hasebe, N., Mori, S., Tagami, T. and Matsui, R. (2003). Geological partial annealing zone of zircon fission-track system: additional constrains from the deep drilling MITI-Nishikubiki and MITI-Mishima. Chemical Geology, 199(1-2), 45–52.

Hueck, M., Oriolo, S., Dunkl, I., Wemmer, K., Oyhantçabal, P., Schanofski, M., Stipp Basei, M.A., Siegesmund, S., 2017. Phanerozoic low-temperature evolution of the Uruguayan Shield along the South American passive margin: Journal of Geological Society, 174 (4): 609-626.

Iñiguez, A. M. and Andreis R. R., 1971. Caracteres sedimentológicos de la Formación Bonete, Sierras Australes de la provincia de Buenos Aires. Reunión Geológica de las Sierras Australes Bonaerenses. Provincia de Buenos Aires. Comisión de Investigaciones Científicas. La Plata. pp. 103-120.

Japas, M.S., 1986. Caracterización geométrico-estructural del Grupo Pillahuincó. I. perfil del arroyo Atravesado. Sierra de Las Tunas, Sierras Australes de Buenos Aires. Academia Nacional de Ciencias Exactas, Físicas y Naturales. Buenos Aires, Anales 38:145-156.

Japas, M.S., 1989. Analisis de la deformacion en las Sierras Australes de Buenos Aires. Anales de la Academia Nacional de Ciencias Exactas, Fisicas y Naturales (Buenos Aires). 41: 193-215.

Japas, M.S., 1995. Evolución estructural de la porción austral del arco de las Sierras Australes de Buenos Aires. Revista de la Asociación Geológica Argentina, 49(3/4): 368-372.

Japsen, P., Chalmers, J.A., Green, P.F., Bonow, J.M., 2012. Elevated, passive continental margins: Not rift shoulders, but expressions of episodic, post-rift burial and exhumation: Global and Planetary Change, V. 90–91, p.73-86.

Juan, R., Jager, J., Russell, J., Gebhard, I., 1996. Flanco Norte de la Cuenca del Colorado. XIII Congreso Geológico Argentino y III Congreso de Exploración de Hidrocarburos. Geología y Recursos Naturales de la Plataforma Continental Argentina. Eds: V.A. Ramos y M.A. Turic. Relatorio 7: 117-133.

Kaasschieter, J.P.H., 1963. Geology of the Colorado basin. Tulsa Geol. Soc. Dig. 31, 177–187.

Kasuya, M., & Naeser, C. W. (1988). The effect of α-damage on fission-track annealing in zircon. International Journal of Radiation Applications and Instrumentation. Part D. Nuclear Tracks and Radiation Measurements, 14(4), 477–480.

Keidel, J., 1916. La geología de las Sierras de la provincia de Buenos Aires y sus relaciones con las montañas del Cabo y los Andes. Min. Agric. Nac., An. Dir. Nac. Geol. Min., IX, 3. Buenos Aires.

Ketcham, R.A., 2003, Observations on the relationship between crystallographic orientation and biasing in apatite fission-track measurements: American Mineralogist, v. 88, p. 817-829.

Ketcham, R.A., 2005, Forward and Inverse Modeling of Low-Temperature Thermochronometry Data: Reviews in Mineralogy and Geochemistry, v. 58, p. 275-314.

Ketcham, R.A., 2011, HeFTy version 1.7.4, Manual.

Ketcham, R.A., Carter, A., Donelick, R.A., Barbarand, J., and Hurford, A.J., 2007a, Improved measurement of fission-track annealing in apatite using c-axis projection: American Mineralogist, v. 92, p. 789-798.

Ketcham, R.A., Carter, A., Donelick, R.A., Barbarand, J., and Hurford, A.J., 2007b, Improved modeling of fission-track annealing in apatite: American Mineralogist, v. 92, p. 799-810.

Ketcham, R.A., Donelick, R.A., Balestrieri, M.L., and Zattin, M., 2009. Reproducibility of apatite fission-track length data and thermal history reconstruction: Earth and Planetary Science Letters, vhufp. 284, p. 504-515.

Ketcham, R.A., Donelick, R.A., and Carlson, W.D., 1999, Variability of apatite fission-track annealing kinetics: III. Extrapolation to geological time scales: American Mineralogist, v. 84, p. 1235-1255.

Kollenz, S., Glasmacher, U.A., Rossello, E.A., Stockli, D.F., Schad, S., Pereyra, R.E., 2016. Thermochronological constrains in the Cambrian to recent geological evolution of the Argentine passive continental margin. Tectonophysics, 716: 182-203.

Kostadinoff, J., 1993. Geophysical evidence of a Paleozoic Basin in the interhilly area of Buenos Aires Province, Argentina. Comptes Rendus XII ICCP. Volumen 1: 397-404. Buenos Aires.

Kostadinoff, J. and Prozzi, C., 1998. Cuenca de Claromecó. Revista de la Asociación geológica Argentina. 53 (4): 461-468.

Kostadinoff, J., 2007. Evidencia geofísica del umbral de Trenque Lauquen en la extensión norte de la Cuenca de Claromecó, Provincia de Buenos Aires. Revista de la Asociación Geológica Argentina. 62 (1): 69-75.

LaTe Andes, 2018. Análisis termocronológico, área off-shore norte. YPF unpublished report

Krob, F.C., Glasmacher, U.A., Bunge, H.P., Friedrich, A.M., Hackspacher, P.C., 2020. Application of stratigraphic frameworks and thermochronological data on the Mesozoic SWGondwana intraplate environment to retrieve the Paraná-Etendeka plume movement. Gondwana Research, 84: 81-110.

Lesta P. and Sylwan, C., 2005. Cuenca de Claromecó. VI Congreso de Exploración y Desarrollo de Hidrocarburos. Simposio Frontera Exploratoria de la Argentina, pp. 217-231. Eds: Chebli, G.A., Cortiñas, J.S., Spalletti, L.A., Legarreta, L., Vallejo, E.L.

Lesta, P., Turic, M. and Mainardi, E., 1978. Actualización de la información de la Cuenca del Colorado. 7° Congreso Geológico Argentino (Neuquén) Actas 1: 701-713.

Llambías E.J. and Prozzi, C. R. 1975. Ventania. 6º Congreso Geológico Argentino. Relatorio 79-102. Buenos Aires.

Loegering, M.J., Anka, Z., Autin, J., di Primio, R., Marchal, D., Rodriguez, J.F., Franke, D., Vallejo, E., 2013. Tectonic evolution of the Colorado Basin, offshore Argentina, inferred from seismo-stratigraphy and depositional rates analysis. Tectonophysics 604, 245–263.

López Gamundi, O.R., Fildani, A., Weislogel, A. y Rossello, E., 2013. The age of the Tunas Formation in the Sauce Grande basin-Ventana foldbelt (Argentina): implications for the Permian evolution of the southwestern margin of Gondwana. Journal of South American Earth Sciences, 45: 250-258

López Gamundi, O.R., 1996. Modas detríticas del Grupo Pillahuincó (Carbonífero tardío-Pérmico), Sierras Australes de la Provincia de Buenos Aires: su significado geotectónico, Revista de la Asociación Argentina de Sedimentología, 3 (1): 1-10.

López Gamundi, O.R., Conaghan, P.J., Rossello, E.A. and Cobbold, P.R., 1995. The Tunas Formation (Permian) in the Sierras Australes Foldbelt, east central Argentina: evidence for syntectonic sedimentation in a foreland basin. Journal of South American Eatrh Sience. 8 (2): 129-142.

Lovecchio, J.P., Rohais, S., Joseph, P., Bolatti, N.D., Kress, P.R., Gerster, R. y Ramos, V.A., 2018. Multistage rifting evolution of the Colorado basin (offshore Argentina): Evidence for extensional settings prior to the South Atlantic opening. Terra Nova, 30: 359-368.

Lovecchio, J.P., Rohais, S., Joseph, P., Bolatti, N.D. and Ramos, V.A., 2020. Mesozoic rifting evolution of SW Gondwana: A poly-phased, subduction-related, extensional history responsible for basin formation along the Argentinean Atlantic margin: Earth-Science Reviews.

Malusà, M.G., and Fitzgerald, P.G., 2019. From Cooling to Exhumation: Setting the Reference Frame for the Interpretation of Thermochronologic Data. In: Fission-Track Thermochronology and its Application to Geology. Eds: Malusà, M.G., and Fitzgerald, P.G. Springer Textbooks in Earth Sciences.

Massabie, A. and Rossello, E. 1984. La discordancia pre-Formación Sauce Grande y su entorno estratigráfico Sierras Australes de Buenos Aires, Argentina. 9º Congreso Geológico Argentino, Actas 1: 337-352.

Mosquera, A., Silvestro, J., Ramos, V.A., Alarcón, M., Zubiri, M., 2011. La estructura de la Dorsal de Huincul, in: Leanza, H.A., Arregui, C., Carbone, O., Danieli, J.C., Vallés, J.M. (Eds.), Geología y Recursos Naturales de La Provincia de Neuquén. Asociación Geológica Argentina, Neuquén, pp. 385–398.

Muir R.A., Bordy E.M., Mundil R., Frei D., 2020. Recalibrating the breakup history of SW Gondwana: U–Pb radioisotopic age constraints from the southern Cape of South Africa. Gondwana Research, 84:177-193.

Pángaro, F. and Ramos, V.A., 2012. Paleozoic crustal blocks of onshore and offshore central Argentina: Newpieces of the southwestern Gondwana collage and their role in the accretion of Patagonia and the evolution of Mesozoic south Atlantic sedimentary basins. Marine and Petroleum Geology. Ed. Elsevier. 1-22.

Pángaro, F., Ramos, V.A. and Pazos, P.J. 2016. The Hesperides basin: a continental -scale upper Palaeozoic to Triassic basin in southern Gondwana. Basin Research 28(5): 685–711.

Rahn MK, Brandon MT, Batt GE, Garver JI (2004) A zero-damage model for fission-track annealing in zircon. Am Mineral 89:473-484

Ramos, V.A., 2008. Patagonia: A paleozoic continental adrift? Journal of South American Earth Sciences. 26: 235-251.

Ramos, V.A., 1999. Evolución tectónica de la Argentina. En Caminos, R. (ed.) Geología Argentina. Instituto de Geología y Recursos Minerales, Anales 29 (24): 715-789, Buenos Aires.

Ramos, V.A., 1984. Patagonia: un nuevo continente paleozoico a la deriva?. 9° Congreso Geológico Argentino (S. C. Bariloche). Actas 2: 311-325. Buenos Aires.

Ramos, V.A., Chemale, F., Naipauer, M., Pazos, P.J., 2014. A provenance study of the Paleozoic Ventania System (Argentina): Transient complex sources from Western and Eastern Gondwana: Gondwana Research 26: 719-740.

Ramos, V.A. and Kostadinoff, J. 2005. La cuenca de Claromecó. Relatorio del 16º Congreso Geológico Argentino. Eds. De Barrio, Etcheverry, Caballé y Llambías. 471-480.

Rapela, C.W., Pankhrust, R.J., Fanning, C.M. and Grecco, L.E., 2003. Basement evolution of the Sierra de la Ventana Fold Belt: new evidence for Cambrian continental rifting along the southern margin of Gondwana. Journal of the Geological Society of London, 160: 613-628.

Reiners, P. W., and Brandon, M. T., 2006. Using thermochronology to understand orogenic erosion. Annual Review of Earth and Planetary Sciences, 34(1): 419–466.

Rossello, E.A., Massabie, A.C., López-Gamundí, O.R., Cobbold, P.R. and Gapais, D., 1997. Late Paleozoic transpression in Buenos Aires and northeast Patagonia ranges, Argentina. Journal of South American Earth Sciences, 10: 389-402.

Rossello, E.A. and Massabie, A.C., 1981. Micro y mesoestructuras en las formaciones Lolen y Sauce Grande y sus implicancias tectónicas. Sierras Australes de Buenos Aires. Revista de la Asociación Geológica Argentina, 36 (3): 272-285.

Ruiz, L. and Bianco, T., 1985. Presencia de restos de Lycopsidas arborescentes en Las Mostazas, Paleozoico Superior de las Sierras Australes, Provincia de Buenos Aires. Primeras Jornadas Geológicas Bonaerenses, Tandil. Comisión de Investigaciones Científicas de la Provincia de Buenos Aires. 217p.

Sellés Martínez, J., 2001. The geology of Ventania (Buenos Aires Province, Argentina). Journal of Iberian Geology, 27: 43-69.

Sellés Martínez, J., 1986. Las Sierras Australes de Buenos Aires: Su vinculación a un cizallamiento regional. Revista de la Asociación Geológica Argentina, 41(1-2): 187-190.

Suero, T., 1972. Compilación geológica de las Sierras Australes de la provincia de Buenos Aires. Ministerio de Obras Públicas, LEMIT, División Geología. Anales 3: 135-147. La Plata.

Tagami, T., Carter, A., Hurford, A.J., 1996. Natural long-term annealing of the zircon fission-track system in Vienna Basin deep borehole samples: constraints upon the partial annealing zone and closure temperature. Chem. Geol., Isot. Geosci. Sect. 130, 147– 157.

Tagami, T., Galbraith, R.F., Yamada, R., Laslett, G.M., 1998. Revised annealing kinetics of fission tracks in zircon and geological implications. Advances in Fission-Track Geochronology. Kluwer Academic Publishing, The Netherlands, pp. 99–112.

Tagami, T. and Shimada, C., 1996. Natural long-term annealing of the zircon fission track system around a granitic pluton. J. Geophys. Res. 101, 8245– 8255.

Tohver, E., Weil, A.B., Solum, J.G. and Hall, C.M., 2008. Direct dating of chemical remagnetizations in sedimentary rocks, insights from clay mineralogy and 40Ar/39Ar age analysis. Earth and Planetary Science Letters, 274: 524-530.

Tomezzoli, R.N., 1997. Geología y Paleomagnetismo en el ámbito de las Sierras Australes de la provincia de Buenos Aires. Tesis Doctoral. Universidad de Buenos Aires, 306 p.

Tomezzoli, R.N., 2001. Further palaeomagnetic results from the Sierras Australes fold and thrust belt, Argentina. Geophysical Journal International 147(2): 356-366.

Tomezzoli, R.N., 2012. Chilenia y Patagonia: ¿un mismo continente a la deriva? Revista de la Asociación Geológica Argentina, 69 (2): 222-239.

Tomezzoli, R.N. and Cristallini, E.O., 1998. Nuevas evidencias sobre la importancia del fallamiento en la estructura de las Sierras Australes de la Provincia de Buenos Aires. Revista de la Asociación Geológica Argentina, 53(1): 117-129.

Tomezzoli, R.N. and Cristallini, E.O., 2004. Secciones estructurales de las Sierras Australes de la provincia de Buenos Aires: Repetición de la secuencia estratigráfica a partir de fallas inversas? Revista de la Asociación Geológica Argentina, 59(2): 330-340.

Tomezzoli, R.N and Vilas, J. F., 1999. Paleomagnetic constraints on age of deformation of the Sierras Australes thrust and fold belt, Argentina. Geophysical Journal International, 138: 857-870.

Uliana, M.A., Biddle, K., Cerdán, J., 1989. Mesozoic extension and the formation of Argentina sedimentary basins. Extensional tectonics Stratigr. North Atl. Margin, AAPG Mem., 46 599–613.

Uriz, N., Cingolani, C.A., Chemale, F.J., Armstrong, R., 2011. Isotopic studies on detrital zircons of Silurian–Devonian siliciclastic sequences from Argentinean North Patagonia and Sierra de la Ventana regions: comparative provenance. Int. J. Earth Sciences 100:571–589.

Varela, R., Dalla Salda, L.H. y Cingolani, C.A., 1985. Estructura y composición geológica de las Sierras Colorada, Chasicó y Cortapié, Sierras Australes de Buenos Aires. Revista de la Asociación Geológica Argentina, 40 (3-4): 254-261.

Von Gosen, W., Buggisch, W. and Dimieri, L.V., 1990. Structural and metamorphic evolution of the Sierras Australes (Buenos Aires Province/Argentina).GeologischesRundschau, 79(3): 797-821.

Von Gosen, W., Buggisch, W. and Krumm, S., 1989. Metamorphism and deformation mechanisms in the Sierras Australes fold and thrust belt (Buenos Aires Province, Argentina). Tectonophysics, 185: 335-356.

Wagner, G.A., and Van den Haute, P., 1992, Fission-track dating: Stuttgart, Enke Verlag - Kluwer Academic Publishers.

Yamada, R., Tagami, T., Nishimura, S., 1993. Assessment of overetching factor for confined fission-track length measurement in zircon. Chem. Geol., Isot. Geosci. Sect. 104, 251–259.

Yamada, R., Tagami, T., Nishimura, S., 1995a. Confined fissiontrack length measurement of zircon: assessment of factors affecting the paleo-temperature estimate. Chem. Geol., Isot. Geosci. Sect. 119, 293– 306.

Yamada, R., Matsuda, T., Omura, K. (2007). Apatite and zircon fission-track dating from the Hirabayashi-NIED borehole, Nojima Fault, Japan: Evidence for anomalous heating in fracture zones. Tectonophysics, 443(3), 153-160.

Zaun PE and Wagner GA (1985) Fission-track stability in zircons under geological conditions. Nuclear Tracks 10:303-307

Zorzano, A., Di Meglio, M., Zavala, C. y Arcuri, M.J., 2011. La Formación Tunas (Pérmico) en la Cuenca Interserrana. Primera correlación entre campo y subsuelo mediante registros de rayos gamma. XVIII Congreso Geológico Argentino, Actas. Neuquén, 2-6.

Highlights

The Ventana Ranges and Claromecó basin, located north of the Mesozoic Colorado basin, record an exhumation history coetaneous with the rifting history of the basin.

Most of the exhumation in the Ventana Ranges and Claromecó basin was achieved during the Mesozoic.

The Ventana Ranges display Late Triassic to Early Jurassic ZFT cooling ages, and Early to Late Jurassic AFT cooling ages.

Permian units in the the Claromecó Basin display Jurassic ZFT cooling ages and Early Cretaceous AFT cooling ages.

A thickness of at least 2,000 m of Permian succession was eroded from the top of the Tunas Fm during the Mesozoic exhumation.

Declaration of interests

☒ The authors declare that they have no known competing financial interests or personal relationships that could have appeared to influence the work reported in this paper.

☐The authors declare the following financial interests/personal relationships which may be considered as potential competing interests: